The H-Pd (Hydrogen-Palladium) System

F.D. Manchester, A. San-Martin, and J.M. Pitre
University of Toronto

Equilibrium Diagram

The Pd-H system is the paradigm of metal hydrogen systems: the longest studied (since 1866 [1866Gra]), the easiest to activate for hydrogen absorption, and probably the richest in the number of physically interesting phenomena that have been observed in this type of system. In matters of the thermodynamics of hydrogen absorption, the details of phase diagram delineation, description and analysis of electronic properties and a number of other features, work on the Pd-H system has tended to provide leading developments that have subsequently been used in other metal-hydrogen systems.

The *T-X* phase diagram (Fig. 1) assessed here for pressures*above 10^2 Pa, consists of the α and α′ phases, in both of which the H occupies, randomly, the interstitial octahedral sites of the fcc Pd lattice. Table 1 gives the crystal structure and the lattice parameters of the system.

The α phase is the low-concentration phase of the system, separated from the high-concentration α′ phase by a mixed (α + α′) phase region. The boundary of this mixed phase region was delineated by taking an average of the limiting *T-X* values for the isotherm plateaus (see Fig. 2) determined by [64Wic], [73Fri], [83Las], [85Las], and [87Wic] from experimental *P-X* isotherms shown in Fig. 3. Because hysteresis** is observed in absorption and desorption isotherms for $T < T_c$ [36Gil, 60Eve, 89Fla], it is possible to draw two different sets of boundaries for the mixed-phase region at each temperature. For clarity, only *P-X* desorption isotherms reproduced from the available literature are displayed in Fig. 3. (See further discussion on locating coexistence boundaries below.)

At ~25 °C, the maximum H solubility in the α phase is $X = 0.017$ (1.68 at.% H), whereas the single α′ phase exists for $X > 0.60$ (37.6 at.% H). The two-phase region in Fig. 1 bounded by the coexistence curve closes at the critical point located at $T = 293$ °C, $X = 0.29$ (22.5 at.% H), and $P = 20.15 \times 10^5$ Pa (see Table 2). There is no distinction between the α and α′ phases above this critical temperature consistent with the applicability of the lattice gas model for the Pd-H system [60Hil, 69Ale, 76Man]. Table 2 compares critical point parameters reported for the Pd-H system. Values obtained by [78Pic] are not included because they lack the overall consistency of those quoted in Table 2, and there is no compelling reason to try to justify this. With the exception of the values from [74Rib1], the critical point parameters have all been observed from analysis of absorption/desorption isotherms only.

[37Lac1] used what amounted to a lattice gas calculation in the Bragg-Williams (i.e. mean field approximation [37Lac2]) to calculate the form of the Pd-H absorption isotherms and, using the Maxwell equal area rule, to determine the location of the α/α′ coexistence curve. [37Lac1] used the experimentally determined location of the critical point (i.e. T_c and X_c [36Gil]) to fix the value of the attractive H-H interaction and the value he assumed for the maximum permitted H concentration. The [37Lac1] calculation, apart from giving the first statistical thermodynamic model for H absorption in Pd-H, provided a parametric relation for analyzing the absorption of H in Pd, which is useful today (see "Solubility"). However, the

*For H-in-metal systems, the equilibrium pressure of the H gas surrounding the metal is always a significant thermodynamic variable, in contrast to most situations involving metallic alloys. Thus, sections of the *P-X-T* surface in a *T-X* plane and a *P-X* plane are always necessary. In the presentation given here, *P* is the pressure in pascals, *T* is the temperature plotted in both K and °C, and *X* is the H concentration expressed either as atomic percent H or as $X = H/Pd$, the atomic ratio.

**Hysteresis in metal-hydrogen systems with mixed phase regions, as in the α/α′ regions of the Pd-H system, arises from plastic deformation due to a large volume change as one phase, e.g. α, changes to the other, e.g. α′, or vice versa (see [89Fla]).

Table 1 Pd-H Crystal Structure and Lattice Parameter Data

Phase	Composition, at.% H	Pearson symbol	Space group	Strukturbericht designation	Prototype	Lattice parameters, nm *a*	*b*	*c*	Comments	Reference
Pd	0	*cF*4	*Fm*3*m*	*A*1	Cu	0.38874	...	...	At 20 °C	[78Kin]
(Pd)	0 to ~2	*cF*8	*Fm*3*m*	*B*1	NaCl	0.3895	...	...	At 25 °C	[64Mae]
α′	~37.6	*cF*8	*Fm*3*m*	*B*1	NaCl	0.4025(a)	...	...	At 25 °C	[64Axe,64Mae]
Low-temperature ordered phases										
A_2B_2	39.9 at.% D	*tI*12 (b)	$I4_1/amd$	C_c	$PdH_{0.5}$	0.402	0.805	1.207	At –230 °C	[78And2] (c)
A_4B	43.2 at.% D	*tI*10	*I*4/*m*	$D1_a$	Ni_4Mo	0.639	0.639	0.404	At –203 °C (d)	[79Ell, 81Bla]

(a) In the literature this has often been referred to as the β^{min} value for the Pd-H lattice parameter [75Sch]. **(b)** This structure is an ordered arrangement of vacancies in the fcc H(D) lattice on interstitial octahedral sites in the Pd lattice. The Pearson symbol has been chosen to count both the vacancies and the interstitial H(D) corresponding to a structure that is stoichiometric at $X = 0.5$ to maintain consistency with the usual listings of this symbol for tetragonal structures. **(c)** Values for lattice parameters of tetragonal cell estimated from [75Sch] with the help of [84Hem] for the *X* value and temperature given by [83Bon]. **(d)** As in (b), except that counting interstitials together with vacancies corresponds to a structure that is stoichiometric at $X = 1$. **(e)** Values for lattice parameters of tetragonal cell estimated from [75Sch] with the help of [84Hem] for the *X* value and temperature given by [79Ell]. The sets of tetragonal lattice parameters referred to in (c) and (e) are for PdD_X.

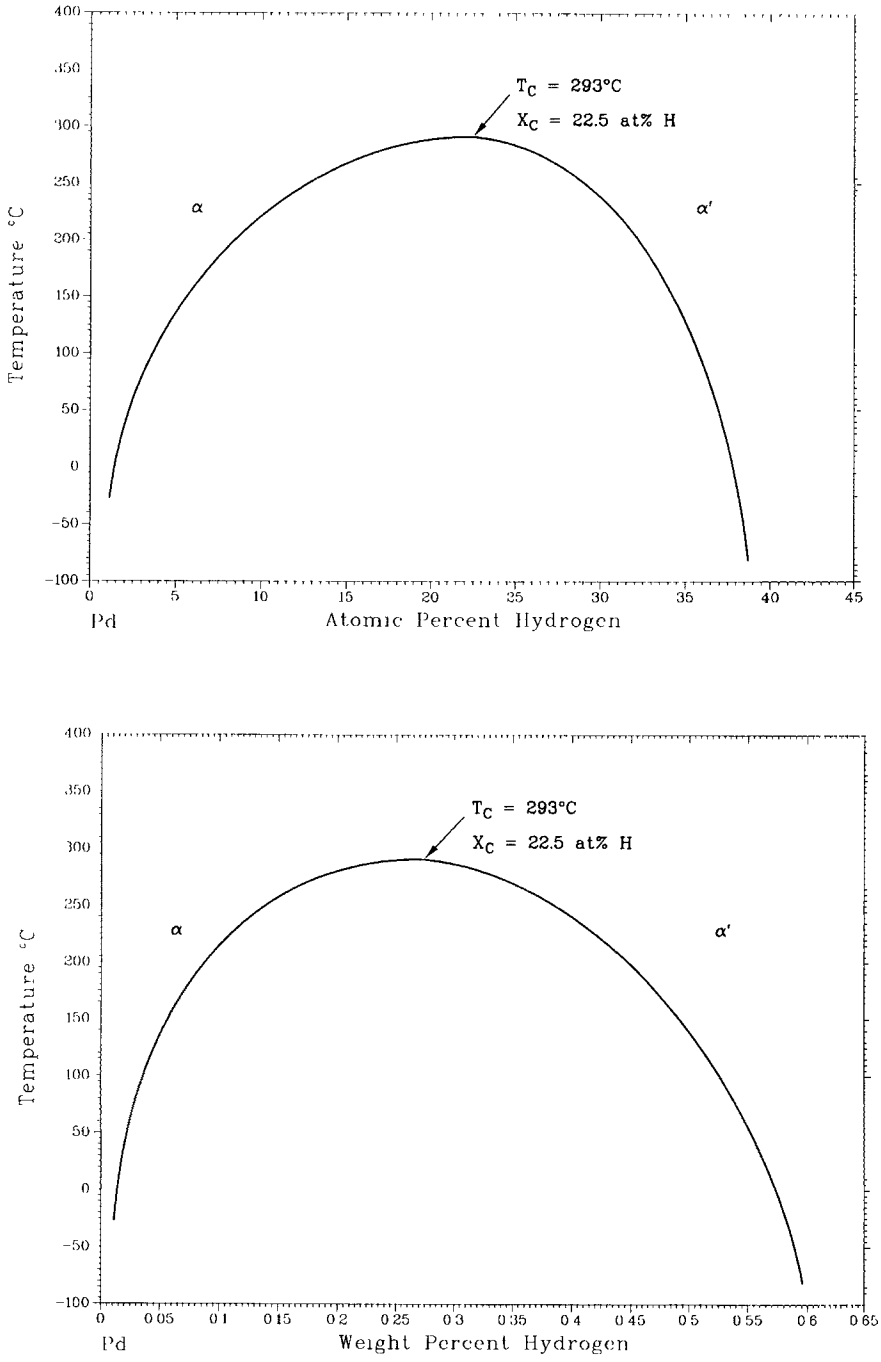

Fig. 1 Assessed Pd-H phase diagram. *T-X* projection from a *P-X-T* surface onto a plane at $P = 10^2$ Pa.

[37Lac1] model was not founded on an assessment of the basic mechanisms responsible for the attractive H-H interaction or on other basic physical features of the Pd-H system. Also using a lattice gas calculation [79Die] estimated values for T_c and X_c and the form of the coexistence curve, which were roughly comparable to those obtained from experiment. [79Die] used a description of the elastic contribution to the H-H interaction, which was based on the earlier work of [74Wag] and [74Hor], and added to this an estimate of the electronic contribution to this interaction. To obtain numerical estimates, [79Die] used experimental data from independent measurements on several basic physical properties of the Pd-H system without reference

to empirical data on the coexistence region. [79Die] suggested that an ability to make more realistic estimates of dielectric screening in Pd-H and more precise experimental data on the strength of the force dipole tensor could improve their theoretical description of the phase diagram for Pd-H in the α/α′ coexistence region.

The existence of ordered phases in the Pd-H system has been observed only* at temperatures below approximately –223 °C, a temperature at which anomalies in various physical properties of the system have been observed [76Jac2] and below which ordering of the interstitial hydrogens has been found [78And1, 79Ell]. The present state of knowledge concerning phase diagram boundaries for ordered structures in the Pd-H system is displayed in the *T-X* diagram of Fig. 4.

Considerable discussion and analysis has been directed at the question of how to best determine the location of the coexistence curve and the values of the critical point parameters from measurements on absorption/desorption isotherms [83Fla, 85Wic, 87Wic]. Much of the discussion concerns the effect of stresses associated with the α/α′ phase transition and how they might influence observation of absorption/desorption isotherms. This question was examined some time ago by [63Sch], who suggested that a desorption isotherm can give a more realistic estimate of the location of the coexistence curve because, with the desorption of only a small amount of hydrogen, the α′ phase would no longer be under stress. Stress free, equilibrium conditions could be considered to apply as desorption proceeded. However, the transmission electron microscope (TEM) investigation of [79Ho] showed that both the growth of α phase in α′ and the growth of α′ phase in α are accompanied by stress and the production of high-dislocation densities (~10^{16}/m^2). The lattice mismatch between α and α′ is ~3% in lattice parameter and ~10% in volume. The variations in microstructure for these processes are moderately complex so that no simple picture of stress relief in desorbing some hydrogen from the α′ phase is available. The TEM evidence supports the solubility evidence of [80Fla] and is consistent with the conclusions of [76Bir] concerning solvus hysteresis in the Nb-H system.

*A possible exception to this statement is the claim by [80Sem] to have observed an ordered structure in a thin Pd-H film at room temperature or above for $X = 1.33$ (see "Crystal Structure").

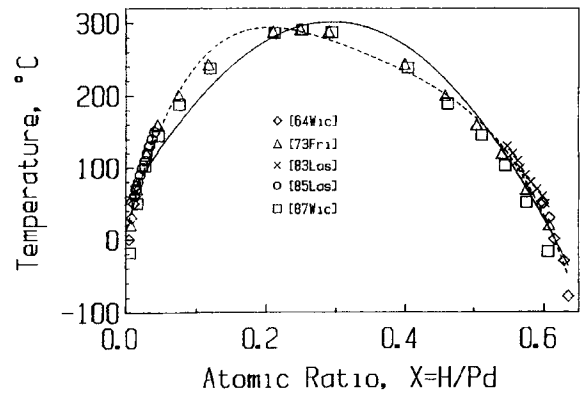

Fig. 2 *T-X* diagram for the Pd-H system with selected data. Dashed line gives a best fit (4th order polynomial) to the limits of the coexistence region as determined by the authors cited. Solid line represents the same data points fitted to a parabola (quadratic trinomial). See text.

For a system such as Pd-H, which is known to satisfy mean field criteria so well, the coexistence curve must be a parabola i.e., critical point exponent, $\beta = 1/2$ [74Rib1]. Critical point exponents are defined in Table 3. As Fig. 2 and 3 show, it is easy to find coexistence region boundaries determined from isotherm data that do not conform very well to a single parabola.

Figure 2 displays the *T-X* values for coexistence boundaries given in tabular form by the original authors. A polynomial fit up to the 4th order (dashed curve) gives T_c and X_c values of 293.7 °C and 0.205, respectively, and follows the data relatively well below a temperature of ~150 °C in both arms of the boundary for the mixed-phase region. The solid curve in Fig. 2 represents a quadratic trinomial fit. Although the values of T_c = 301.2 °C and $X_c = 0.295$ obtained from this fit are close to the assessed critical values (see Table 2), the fitted parabola deviates considerably from the data points in the low-concentration arm of the boundary. The phase boundaries for the mixed-phase region in Fig. 3 (dashed and solid lines) were obtained by mapping the corresponding lines of Fig. 2 into Fig. 3.

[87Wic] compared coexistence region boundaries obtained solely from desorption isotherms with those obtained solely from absorption isotherms in a test aimed at demonstrating that data from desorption isotherms are to be preferred in locating the best value for X_c, the critical concentration. However, in making a choice between the two coexistence curves, it is difficult to find a reconciliation between a parabolic fit to each of the curves and a unique critical temperature for these data. Thus, on the basis of currently available information, stress accompanying the α/α′ transformation for both absorption and desorption isotherm determinations is likely to hamper attempts to obtain a good representation of the coexistence curve and of the values of critical point parameters for a Pd-H

Table 2 Critical Point Parameters for the Pd-H System

References	P_c, Pa × 10^5	X_c, H/Pd	T_c, °C
Pd-H			
[36Gil] (a)..	20.1	0.270	295 3
[73Fri]..	20.0 ± 0.2	0.250 ± 0.005	291 ± 2
[74Rib1]	20.15 ± 0.05	0.29 ± 0.01	293 ± 1
[86Fen1]	20.1 ± 0.15	0.26 ± 0.005	295 ± 1
[87Wic]	19.9 ± 0.2	0.257 ± 0.004	290 ± 1
Pd-D			
[87Wic]	39.0 ± 0.5	0.257 ± 0.004	283 ± 1

(a) These values are quoted as being the earliest assignments of critical point parameters reasonably compatible with more recent results. No explicit description of the parameter determinations was given by [36Gil].

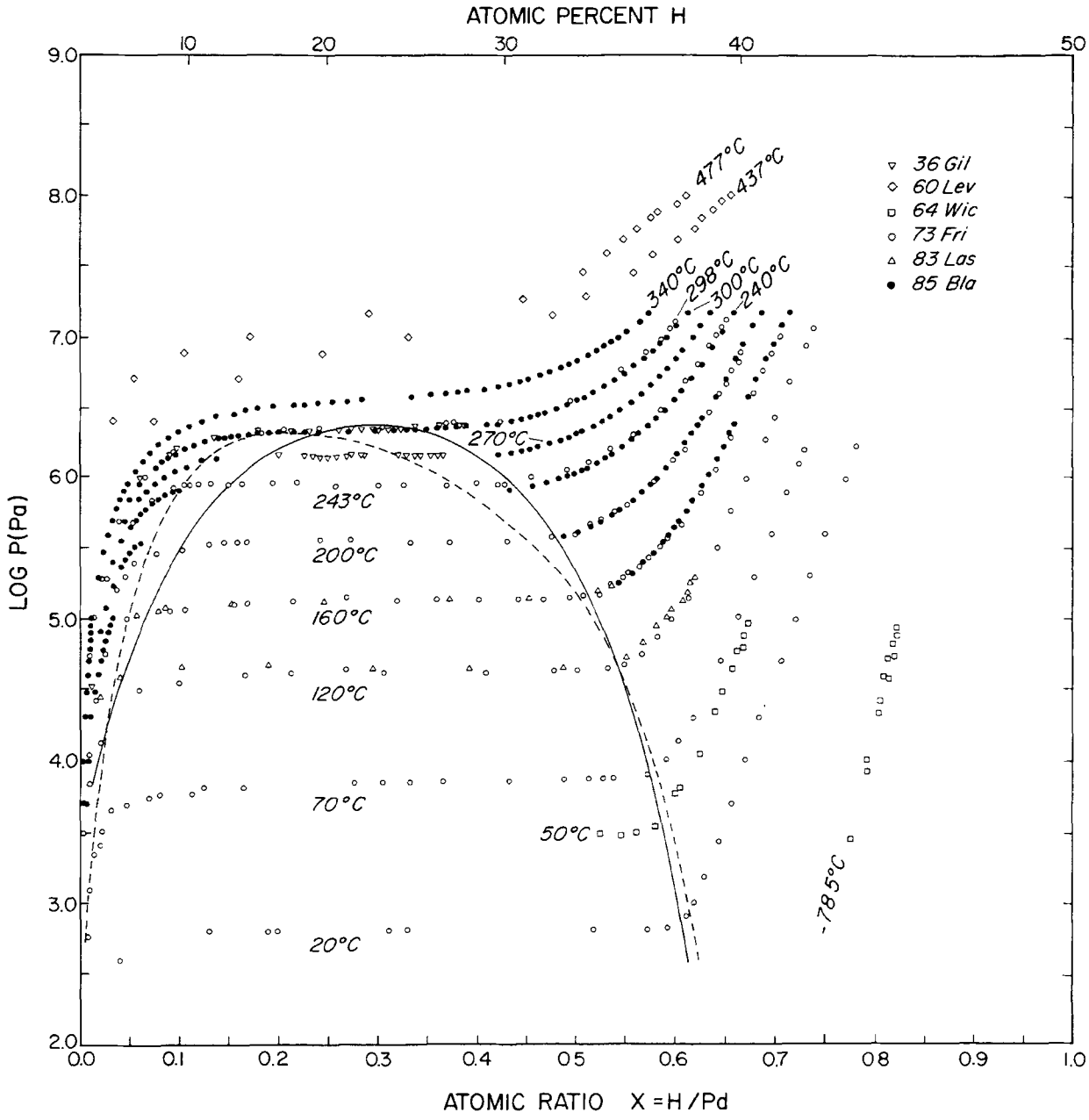

Fig. 3 Pressure vs composition isotherms for the Pd-H system. A representative selection of isotherms are shown. Data for all isotherms that show points in the coexistence region were measured in desorption, as were those for [60Lev] and [64Wic]. For designation of solid and dashed lines, refer to Fig. 2.

system in equilibrium. It would seem that using several different types of physical measurement, with each one chosen to yield values for critical point parameters, then optimizing their internal agreement would offer the best hope of improving precision in the location of the critical point for the Pd-H system and similar systems.

A first step in this direction was taken by [74Rib1], who attempted to achieve compatibility between data based on isotherm measurements and data obtained from Δ_E, the relaxation strength for the elastic after-effect (Gorsky effect). This compatibility was achieved under the constraint of having the critical point exponent, γ, $\{\Delta_E \alpha(T - T_c)^{-\gamma}\}$—(see Table 3)

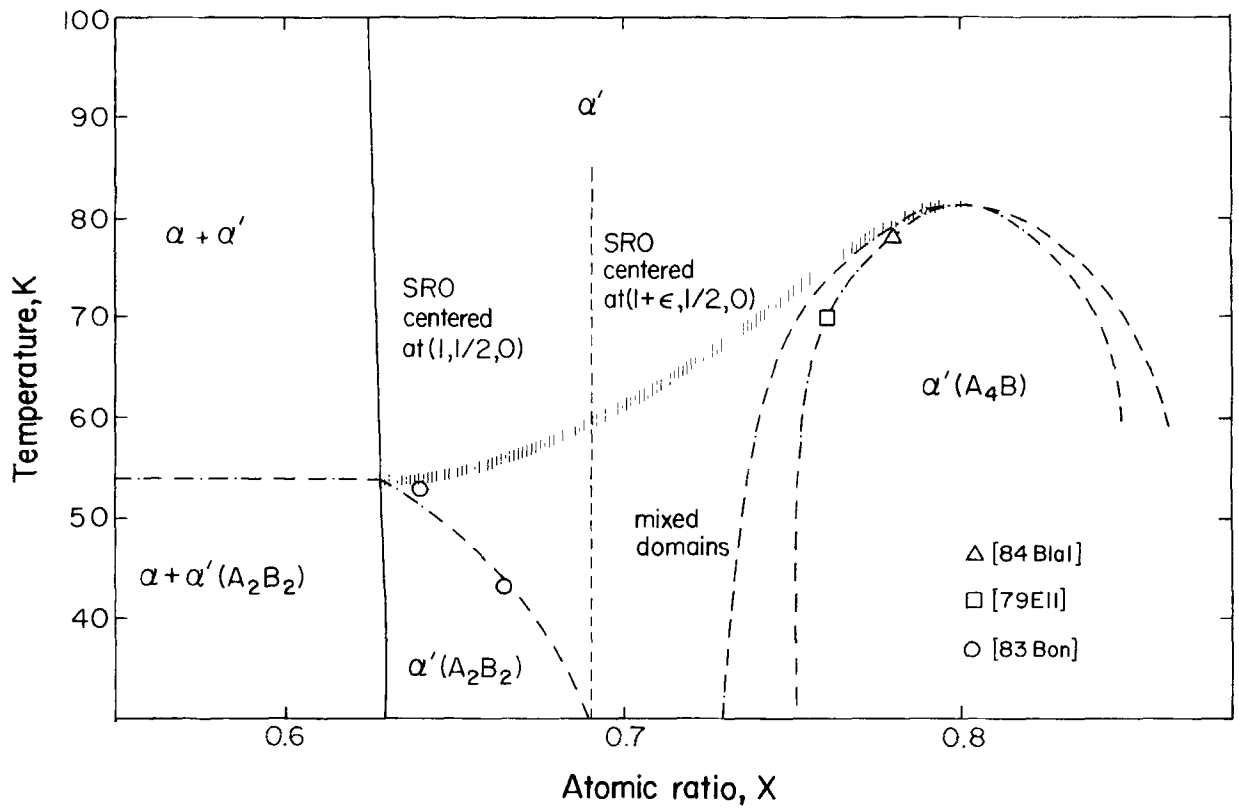

Fig. 4 *T-X* diagram for the high-concentration, low-temperature region based on [82Bon] and [84Bla2], with added experimental information (see text). Phase boundaries are indicated by solid lines; onset of ordering by dot-dashed lines; the approximate location of the "50 K anomaly" by the hatched curve. Equilibrium pressures are not available for this low-temperature part of the phase diagram.

Table 3 Critical Point Exponents for H in Pd System (a)

Exponent	Mean field value	Experimental value	Relevant physical quantity	Exponent relation
Static measurements				
α	0 (discontinuity)	0 (discontinuity)	Specific heat	$C_v \sim (T - T_c)^{-\alpha}$
β	½	0.55 ± 0.05	Coexistence curve	$\rho - \rho_c \sim (T - T_c)^{\beta}$
β_s	½	0.55 ± 0.05	Spinodal curve	...
γ	1	1.01 ± 0.1	Compressibility	$K_T \sim (T - T_c)^{-\gamma}$
		1.02 ± 0.04 (b)	...	$\Delta_E \sim (T - T_c)^{\beta}$
δ	3	3.2 ± 0.3	Critical isotherm	$P - P_C \sim (\rho - \rho_c)^{\delta}$
Dynamic measurements				
Δ	1	1.01 ± 0.1	Relaxation time	$\tau \sim (T - T_c)^{-\Delta}$

Note: T_c is the critical temperature. ρ_c is the critical density. P_c is the critical pressure. **(a)** From measurements of [74Rib1]. **(b)** For Pd-Ag-H alloys from [72Buc].

compatible with the other critical point exponents for the Pd-H system, all of which conform to mean field values (see Table 3). The conformity with mean field values is a consequence of the attractive, long-range, lattice-mediated, hydrogen-hydrogen interaction, which is the dominant influence for the critical point transition of the Pd-H system [37Lac2, 73Hal].

Because these more general features of the critical point transition were taken into account, we recommend the adoption of the [74Rib1] values (see Table 2) for the critical point parameters for the Pd-H system. We also recommend that further experimental work be done on improving the determination of the critical point parameters, using and possibly extending the general approach of [74Rib1].

The incoherent spinodal for this system determined experimentally by [75Rib] is shown in Fig. 5. [75Rib] determined also that both the coexistence (outer) curve and the spinodal

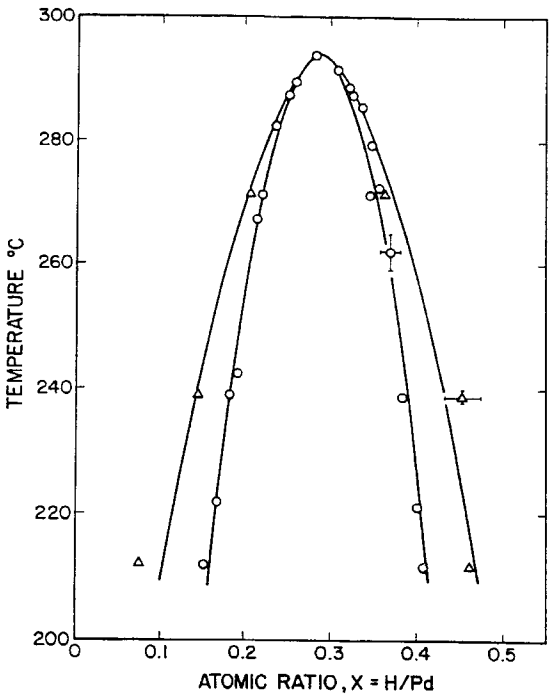

Fig. 5 Experimental spinodal curve for Pd-H. From [75Rib]. The spinodal, which is the incoherent spinodal [62Cah1], is shown inside the coexistence curve for the α/α' transformation.

(inner) curve of Fig. 5 were symmetric to X_c, with a critical point exponent $\beta = 0.55 \pm 0.05$. This result, together with other experimental values of critical point exponents (see Table 3), were obtained by [74Rib1] and [74Rib2] for a range of measurements for which $t > 10^{-3}$ [$t = (T - T_c)/T_c$]. The locations of coherent spinodals in the T-X plane have been calculated for a thin PdH_X disc [92San]. Coherent nucleation of α phase in α' phase and vice versa was reported in the TEM observations of [79Ho].

Equilibrium Pd-H Phase Diagram In Restricted Geometries

A number of absorption/desorption isotherms have been measured for H in Pd samples with one dimension of ~10 to 100 nm. Most of this work [74Buc, 79Fra, 80Fra, 83Bak, 83Fee, 86Fee2, 87Sal] has been with Pd films evaporated onto a quartz substrate, whereas in one case [79Eve], H absorption was studied in Pd black, for which the crystallite dimensions were comparable to the film thicknesses cited above.

[83Bak] and [83Fee] gave as their motivation for studying this system the prediction of [72Ale] that the strength of the H-H interaction in an M-H system of finite size should depend on the elastic conditions that hold at the boundary of that system. They regarded H in a deposited Pd film as giving a system that was considerably clamped by the adherence of the film to the substrate, enough, they estimated, to reduce the strength of the attractive H-H interaction and thus to lower the critical temperature, T_c, and reduce the width of the α/α' coexistence region by a measurable amount from the values that apply for a bulk sample. No motivation stated so far has been concerned with studying the Pd-H phase diagram for a sample that was essentially two dimensional, and the relationship between dimensionality and the character of the critical point transition [77Als]. For such a study, the boundary conditions for a thin film would have to be carefully prescribed.

A variety of techniques for measurements on the thin films have been used, the most common being that of the piezoelectric quartz crystal microbalance (PQCM) [74Buc, 80Fra, 83Fee]. Alternative techniques were a volumetric method equivalent to that conventionally used for absorption/desorption isotherms [85Lee] and a gravimetric method using a microbalance [86Fee1] employed by [86Fee2].

The results from measurements using the PQCM showed considerable variation. For example at 300 K, the plateau width was observed to be the same as that for bulk Pd-H [80Fra], narrower [83Fee], or wider [74Buc], for films that had comparable thicknesses. Earlier work [72Eer, 74Buc] showed that the frequency changes of the PQCM were not just simple functions of the extra mass loading of the crystal. For the loading of interstitial H into the Pd film, internal strains in the film could also contribute to frequency changes. Other factors can come into play on the introduction of H into the Pd film. There are possibilities of changes in mechanical characteristics, such as acoustic coupling and the degree of detachment of the film from the quartz surface. Also, the role that the particular cut of the quartz crystal plays in some of these effects is still not well understood.

Two attempts [85Lee, 86Fee2] to examine the relationship between film thickness and absorption isotherm characteristics, without the uncertainties of the PQCM technique, have produced more definitive evidence of changes in the isotherms but have not determined the exact causes of these changes. Both investigations showed that for film thicknesses of 50 nm and below there is a narrowing of the coexistence region with respect to that for bulk samples, and [86Fee2] quoted a drop of 26 K in the critical temperature for a 50 nm PdH_X film. As a measure of the decrease in the extent of the coexistence region, [85Lee] plotted the change in hysteresis loop area with film thickness and noted the similarity to a plot constructed from the results of [79Eve], in which film thickness was replaced by the size of crystallites in the samples they used for isotherm measurements on Pd black. Considering the results of [79Eve], [85Lee], and [86Fee2] together, experimental evidence shows that in PdH_X systems for which the grain size or crystallite dimensions have been reduced to 50 nm or less, there is a lowering of the coexistence region and the critical point temperature as described above and therefore that restricted geometries do have an effect on the character of the phase diagram. However, whether the observed changes are simply due to the effect of restricted geometries on the H absorbed interstitially in the Pd or are the result of one or more of the mechanisms considered by [85Lee] and [86Fee2] particularly, remains to be established.

Solubility of H in Pd

Sieverts' law ($X \propto P^{1/2}$) is obeyed in liquid [80Kal] and in solid Pd at low-hydrogen concentrations [29Sie, 64Wic, 65Sim,

73Cle, 74Eva, 79Lew, 80Kal, 83Las, 84Las, 85Las, 86Las]. According to [73Bur], deviations from this law appear at $T <$ 250 °C and $X > 0.006$ (~0.6 at.% H).

The solubility decreases as the temperature increases, and at the melting temperature of Pd, the transition from solid to liquid is marked by a positive step in the solubility (see Fig. 6). The H solubility increases at high hydrogen pressures (see "α′ Phase") and also as a result of the creation of dislocations in the Pd matrix (see below).

The presence of impurities on the surface of Pd dramatically affects the hydrogen absorption. Thus, early solubility measurements at temperatures below 120 °C [60Eve] were performed on finely divided Pd, which presented a very active surface for the hydrogen dissociation. *P-X* equilibrium measurements on bulk Pd, at temperatures around –80 °C were possible only by covering the Pd surface with a hydrogen-transfer catalyst [64Wic] or by using ultrahigh vacuum (UHV) techniques to maintain a high degree of cleanliness on the Pd surface during solubility measurements [73Cle]. Other techniques used for absorbing hydrogen in Pd, apart from the gas loading method, include: the tungsten filament method [15Lan, 62Bon, 75Oat], the gas discharge method [52Nor], the H ion implantation method [72Str], and the electrochemical method [67Lew].

The absorption of H in a metal has usually been measured with a gas volumetric technique in which the volume of absorbing H gas is metered to the metal sample contained in an experimental chamber fitted with an absorption pressure monitor. Historically, the absorption of H in Pd was the first measurement of this type (e.g. [10Sie]). Modern versions of this type of apparatus are often automated and can employ gravimetric determination of the amount absorbed by means of a microbalance (e.g. [89Ben]). Other means used to follow H absorption (usually isotherms) include: measurement of sample dilation [74Rib1, 86Fee1] and change in resonant frequency of a quartz crystal as a result of H absorption in a Pd film for which the crystal is acting as a substrate [74Buc]. Electrical resistance measurements have been used to follow H absorption isotherms in Pd [33Bru, 50Wri], but this has not been developed into a generally useful technique because the links between H absorption and electrical resistance are relatively complex. Complexity of linkages is also a problem for the quartz crystal method.

α Phase

A large number of measurements of H solubility in the α phase of Pd-H have been made over the years. As the measurements were refined and the preparation and characterization of the Pd samples improved, it became evident that H solubility measurements on fine powders used in the earlier and some later work, including those on "Pd black" (a loosely defined term for Pd in a fine powder form), were affected by H adsorption on the surfaces of the fine powder grains. Typically, these powders had adsorption surface areas of ~1000 m^2/kg, and estimates [68Abe] indicated that the number of adsorbed H atoms was approximately equal to the number of surface Pd atoms. Thus measurements of the absorption of H in the Pd lattice, at low concentrations, could be seriously misrepresented unless a correction was made for surface adsorption effects [74Eva, 79Eve]. There have been a number of H solubility measurements made on Pd in the form of a bulk solid, i.e. foils or wires, for which the H adsorption corrections were essentially negligible (surface areas of the order of 1 m^2/kg) [64Wic, 65Sim, 73Bur, 73Cle, 74Eva, 76Bou1, 76Bou2, 78Pic, 84Las], and from these, we have selected data as discussed below. The

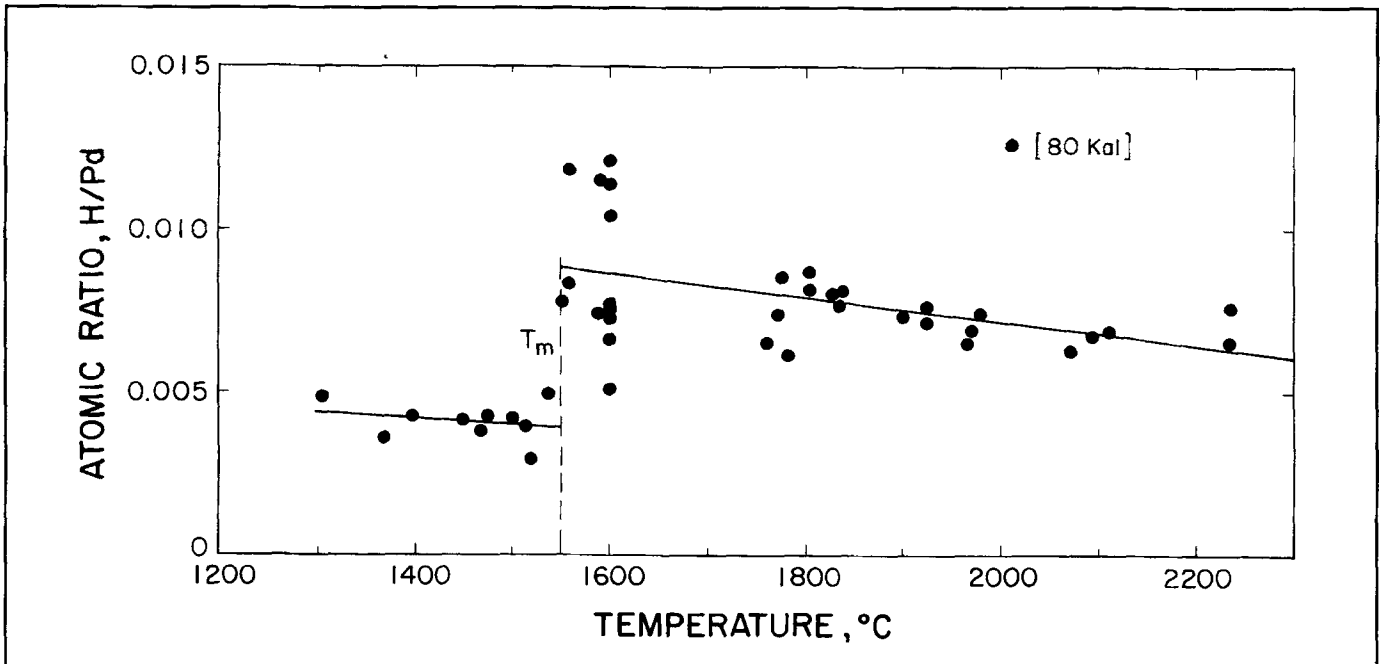

Fig. 6 Solubility of H in Pd in the vicinity of the Pd melting point at $P(H_2) = 0.1$ MPa. Straight line fits are for estimating the solubility jump and do not represent an attempt to describe the $X(T)$ dependence.

early analysis of [37Lac1] provided an analytic relationship for Pd-H isotherms that has often been used for presenting H solubility data in parametric form, particularly at low H concentrations. This same relationship, of course, expressed the physics of the absorption of H in Pd, being based on a calculation (the Bragg-Williams model, in the mean-field approximation) that took into account one of the prominent features of the Pd-H system: that the H-H interaction was of very long range, a concept reinforced by later work [75Rib]. Using the form of the Lacher isotherm equation, the equilibrium H pressure may be expressed by:

$$\ln P = C_1 + C_2/RT + C_3X/RT + 2\ln(X/1 - X) \qquad \text{(Eq 1)}$$

where the C's have been related to the entropy (C_1), enthalpy (C_2), [37Lac1, 64Wic, 65Sim], and the H-H interaction energy (C_3) [37Lac1, 60Hil, 75Rib], for H absorbed in Pd.

We used Eq 1 to represent H absorption in the Pd-H α phase for all the sets of solubility data we selected [64Wic, 65Sim, 73Bur, 74Eva, 84Las], spanning the temperature range from 0 to 450 °C. The Pd samples used to give the selected data were all in bulk metal form: i.e. Pd sheet [64Wic], Pd wire [65Sim, 73Bur, 84Las], and Pd foil [74Eva]. We have used a form of Eq 1 that is more convenient for this purpose, i.e.:

$$\ln[P^{1/2}(1 - X)/X] = A + BX/T \qquad \text{(Eq 2)}$$

In this form, A has an inverse temperature dependence, and we found this to be close to linear over the range of the selected data, as shown in Fig. 7 and for which, with the pressure expressed in atmospheres, (i.e. in units of 11.013×10^5 Pa), we quote the least squares fit:

$$A = (6.086 \pm 0.041) - (1030 \pm 16) \times (1/T) \qquad \text{(Eq 3)}$$

All the selected experimental values were given equal weight in obtaining this fit. For B, we also found a dependence on the inverse temperature that we assumed to be linear and of the form:

$$B = -M/T \quad \textit{with}\ M = (1970 \pm 90) \times 10^3 \qquad \text{(Eq 4)}$$

for which the high-temperature form is at least consistent with B (equivalent to C_3 in Eq 1) representing the H-H interaction in the Pd-H system. Except for the case of [65Sim], we did not have the original experimental data to work from but were restricted to digitized representation of published plots. In the course of assembling the data for the plot of Fig. 7, we found that the 25 °C solubility data of [65Sim], as reported, were not consistent with the rest of their data, so we did not include their 25 °C data. We also found that the values for A, obtained by [74Eva], were misquoted in Eq 5 of his paper; we give the correct values in the plot of Fig. 7.

If we incorporate the above temperature dependencies in the isotherm equation (Eq 2), we find that for P expressed in pascals, we get:

$$\ln P = (23.70 \pm 0.08) - (2060 \pm 30)/T - (3940 \pm 200) \times 10^3 \cdot X/T^2 + 2\ln[X/(1 - X)] \qquad \text{(Eq 5)}$$

for temperatures between 0 and 450 °C. Using Eq 5, we calculate the equilibrium H_2 pressure for a value of X = H/Pd = 0.01, for example, to within a discrepancy that is typically ±15% of the value interpolated from individual pressure measurements of the original sets of selected experimental data listed above. In its present form, Eq 5 is marginally useful, but it is an indication that straightforward improvements in data gathering could produce a $P(X,T)$ relation that could be very useful for the α phase region of the Pd-H system.

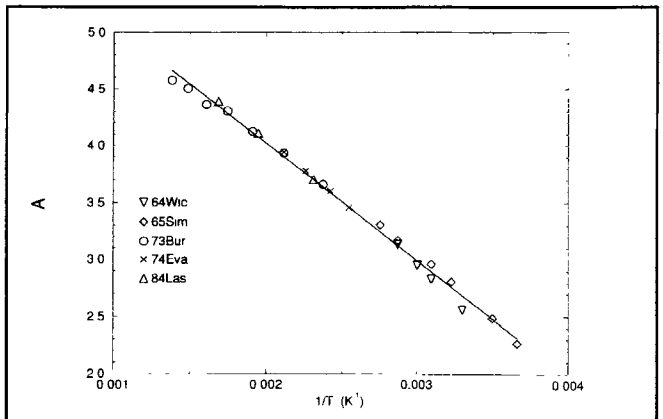

Fig. 7 Straight-line fit to the temperature variation of A, the parameter in the Lacher isotherm relation (Eq 2). Points were taken from selected solubility measurements in the α phase region.

Solubility measurements in cold-rolled Pd samples showed an increased H solubility [75Fla1, 73Fla3, 81Sak] over that of annealed metal. Data from [76Fla1] indicated that for cold-rolled samples, the $\alpha/(\alpha + \alpha')$ phase boundary in the T-X diagram of Fig. 1 moves, at 20 °C, from $X = 0.0085$ to $X = 0.017$ (~0.84 to 1.7 at.% H). Control measurements with well-annealed samples [75Fla1, 76Fla1] were found to be in excellent agreement with early solubility data [64Wic, 65Sim, 73Cle]. [75Fla1] and [76Fla2] verified that vacancies do not play a direct role in the solubility enhancement, but that within the range of deformations studied, the enhancement was directly proportional to the volume of deformation. This led [75Fla1] and [76Fla2] to invoke the strain field of the dislocations to explain the results. The model developed by [76Fla2] fitted the experimental value of the solubility enhancement for a sample deformed 78% (by cold rolling) if a uniform dislocation density of 9×10^{15} m^{-2} and a core radius r_o of $2b$ (b is the Burgers' vector) were assumed. Later, [80Tys] in reexamining the results of [76Fla1], introduced an "extended core" model, in which most of the solubility enhancement occurs in a volume around the dislocation, between r_o and an outer radius R. [80Tys] assumed values of $r_o = 10b$ and $R = 21.2b$, corresponding to a dislocation density of 10^{16} m^{-2}, consistent with a deformation of 78% used in the experiments of [76Fla1], and also assigned a value for the hydrogen-dislocation interaction energy. With these parameters, [80Tys] obtained an improved fit to the [76Fla1] results including the temperature dependence of the enhanced solubility.

Further measurements of the role of dislocations in the enhancement of H solubility in deformed Pd were made by [81Kir1] for H concentrations down to $X = 10^{-6}$, or two orders of magnitude below the concentration range used by [76Fla1]. This difference in concentration range is important because at the lowest H concentrations sampled, deep trap sites close to a dislocation appear not to be filled. Concomitantly, very high

Table 4 Selected Values of the Enthalpies (ΔH) and Entropies (ΔS) of the Pd-H System for H Absorption ($\alpha \rightarrow \alpha'$) and Desorption ($\alpha' \rightarrow \alpha$) Processes

Transition	Method	$\lvert\Delta H\rvert$ kJ/0.5 mol H_2	$\lvert\Delta S\rvert$ J/0.5 mol H_2 · K	Reference
$\alpha \rightarrow \alpha'$	Calorimetry	19.09 ± 0.10	46.6	[91Fla]
	van't Hoff plot	18.7 ± 0.15	46.3 ± 0.4	[83Las]
$\alpha' \rightarrow \alpha$	Calorimetry	19.28 ± 0.13	46.6	[91Fla]
	van't Hoff plot	19.5 ± 0.25	46.2 ± 0.6	[83Las]
Average $\lvert\Delta H\rvert$	Calorimetry	19.2	...	[91Fla]
	van't Hoff plot	19.1	...	[83Las]

Note: The calorimetry results were obtained in the temperature range $333 < T < 433$ K.

values of H solubility enhancement were observed in this concentration range, e.g. $X_d/X_u = 1.2 \times 10^6$ for a deformation of 73% at $X = 10^{-6}$ (X_d and X_u are the H concentrations in the deformed and undeformed Pd samples evaluated at the same H_2 pressure). The electrochemical cell emf's for deformed and undeformed Pd samples could be used as a measure of their chemical potentials through the use of the Nernst equation. For the low-concentration conditions, the chemical potential for the deformed samples could be compared with a calculated chemical potential. For the region experiencing elastic stress close to the dislocation, the site densities can be treated using a Fermi-Dirac distribution [56Lou, 58Bes, 67Fio, 78Hir] as the sites involved can be regarded as having unique energies in this stress field, and the situation becomes one of distributing identical particles over an assembly of discrete energy states. A plot of the chemical potential of the H interstitials in the undeformed Pd (their "Fermi-Dirac" energy) against $(X_d)^{-1/2}$ supported the [81Kir2] analysis of the elastic interaction between H interstitials and the stress field of the dislocations and also showed that there was an extra contribution to the interaction energy that could be attributed to the formation energy of a close aggregation of H on the sites near the dislocation. The estimate of this energy [82Kir] was close to the value of the enthalpy of formation $\Delta H_{\alpha \leftrightarrow \alpha'}$ (see Table 4). There are a number of qualifications and conditions pertaining to this result. For example, only an edge dislocation in an elastic continuum approximation was considered in estimating the elastic contribution to the chemical potential. However, the principal features of the [81Kir2] analysis appear to be supported by experiment [81Kir1, 82Kir] and give a microscopic mechanism for the interaction between H interstitials and the stress field surrounding a dislocation in Pd. Over the concentration range above $X = 10^{-4}$, the measurements of the enhancement of H solubility with sample deformation of [81Kir1] and [76Fla1] were in agreement (see Fig. 8), and the proportionality of the H activity in deformed Pd to the H concentration was also established.

Solubility enhancement is also produced by the transformation from α to α' phase (and vice versa, see "α' Phase"). [77Lyn] estimated from their solubility measurements that a dislocation density of $\sim 5 \times 10^{16}$ m^{-2} was needed to explain the observed solubility enhancement. Results of internal friction measurements [67Aro, 76Jac1, 81Maz] are consistent with the production of very large numbers of dislocations by the α/α' transformation. Direct evidence of the high number of dislocations generated by the α/α' transition is available from TEM observations [72Wis, 76Jam, 77Ho, 79Ho].

Formation of the α phase was studied [76Jam, 77Ho, 79Ho] by following the transformation from α' to α phase under the electron microscope. At room temperature, only the dendritic precipitation of α phase in the α' phase matrix was observed [79Ho] in samples with $X = 0.3$ and 0.6 (23 and 37.5 at.% H, respectively). On cooling rapidly to ~ 90 K (–180 °C), which is estimated by [79Ho] to be lower than the temperature of the coherent solvus at $X = 0.6$, two different morphologies for the precipitation of α phase in α' phase were found [77Ho, 79Ho] in specimens with $X = 0.6$. These were coherent, lenticular, α platelets lying on {100} planes of the α' phase matrix and incoherent α precipitates that eventually formed dendrites with ⟨100⟩ growth axes. The coherent platelets, at least initially, had no dislocations inside them but some nucleated dislocations during growth, predominantly within the platelets, and subsequently grew into large incoherent precipitates, again with dendrite morphology. Coherent platelets that did not nucleate dislocations eventually dissolved back into the α' matrix, even with the temperature essentially constant. Similar behavior was observed for α' nucleating in α (i.e. for a sample with $X = 0.05$) and an important feature of the TEM observations was the evidence that high-dislocation densities could be produced as a result of the α/α' transition proceeding in either direction, contrary to the suggestion of [63Sch]. These observations were made possible by the production of high-concentration Pd-H samples with low-dislocation densities as a result of using gas loading and avoiding the α/α' mixed-phase region. The {100} habit planes correspond to the predictions of [62Cah2] for precipitates resulting from spinodal decomposition in cubic systems, although the experimental observations reported by [79Ho] were for coherent nucleation only.

α' Phase

The absorption of H, under isothermal conditions, to concentrations beyond the $\alpha + \alpha'/\alpha'$ phase boundary requires, in general, equilibrium pressures that are significantly above atmospheric (see Fig. 3); thus measurements of physical properties of the α' phase have been made for H pressures in the GPa region (see below). Other methods have been used also to provide an effective chemical potential that is equivalent to that for H at high pressures. These include the tungsten filament method [75Oat], the method of lowering the temperature during electrolytic charging in selected electrolytes [74Har], and

the use of ion implantation at 4 K (–269 °C) [72Str]. With all of these methods, H concentrations close to $X = 1$ have been claimed with varying degrees of substantiation [75Oat]. Ion implantation at low temperatures is least likely to provide a sample with a homogeneous H distribution, but for some experiments on superconductivity in Pd-H, this was not a major concern.

Figure 3 includes two isotherms from [60Lev] measured at temperatures above the critical temperature and covering a pressure range from 5 to 100 MPa (50 to 1 kbar). Both curves indicate a continuous increase of the H absorption with increasing pressure. The highest X value reported by [60Lev] amounted to 0.690 (40.83 at.% H) at $T = 326$ °C and $P = 100.3$ MPa. Measurements from [52Per] (also not included in Fig. 3) gave for $P = 70.9$ MPa, H contents at 15 °C of 0.876 (46.70 at.% H) and at 88 °C of 0.774 (43.63 at.% H), respectively. [52Per] reported a linear relationship between the measured X values and the logarithm of the H pressure similar to the relation suggested for the –78.5 °C and the 50 °C isotherms from [64Wic] in Fig. 3.

Complete occupation by H of all octahedral interstitial sites in the fcc Pd lattice corresponds to $X = 1$. A number of claims reporting $X > 1$ for H in bulk samples of Pd have been made [69Bar, 71Wis, 78Bar], but some of these have been contested [79Kep] and none of them so far have been unequivocally substantiated. More recently, however, use of the diamond cell has enabled pressures in the GPa region to be applied to Pd-H and Pd-D samples. Using this technique, [89Hem] obtained stoichiometric PdH and PdD and [90Sil] loaded D into Pd to the $X = 1.34$ level (at pressures of 10.5 GPa). Claims have also been made of obtaining $X > 1$ for more specialized conditions. [72Str] claimed the possibility of values up to $X = 1.2$ in Pd films subjected to H ion bombardment but admitted that there was a possibility of significant error in their estimate. [80Sem] claimed to have obtained $X = 1.33$ for H in films of Pd with thicknesses in the range of 50 to 100 nm (see "Crystal Structures and Lattice Parameters"). The question of the limiting value of X and the related question of tetrahedral interstitial site occupation simultaneously, or on completion of occupation of octahedral sites in the fcc Pd lattice, was intensively reexamined recently. This was in response to speculation [89Fle, 89Jon] that a process analogous to muon catalyzed fusion [86Jon] could occur with deuterium absorbed in a Pd lattice. Analysis of the possibilities for minimum separation between hydrogens (deuteriums) in the Pd lattice [89Ric, 89Sun, 90Wei, 91Swi] based on the fairly detailed knowledge of the Pd-H(D) and H-H(D-D) potentials now available, gave results consistent with octahedral occupation only and H-H(D-D) separations significantly greater than the equilibrium separation in a molecule of H_2 or D_2 (for H_2 and D_2 the interatomic distance is 0.074 nm). This separation is far greater than any threshold distance for a nuclear fusion reaction. Experimentally, no H occupation of tetrahedral interstitial sites has been confirmed and no H-H(D-D) separation less than the criterion of 0.21 nm [79Swi], has been reliably reported for the Pd-H system. [90Sil] found no experimental indications of nuclear fusion in $PdD_{1.34}$ over the temperature range 4.3 to 400 K, at pressures of up to 10.5 GPa provided by a diamond anvil cell. They employed detectors for neutron production (detection limit: 2.5×10^{-18} fusions (DD pair)$^{-1}$ s^{-1}); heat production (limit 1.5×10^{-8} fusions (DD pair)$^{-1}$s^{-1}) and gamma ray emission (no gamma rays above background).

Low-Temperature Ordered Structures

The existence at temperatures in the range of $40 < T < 85$ K of two ordered structures designated in the literature by space groups $I4_1/amd$ and $I4/m$ (A_2B_2 and A_4B in Fig. 4) was first established by the neutron diffraction (ND) experiments of [78And1] and [79Ell], respectively. Anomalies, which turned out to be related to these ordering transitions particularly the transition to the A_2B_2 structure, had been reported earlier for the specific heat [57Nac, 63Mit, 77Jac], electrical resistivity [60Sch, 68Ho, 68Hay, 68Sko, 69Ho], Hall effect [71Zep], and later on, thermal expansion coefficient [84Gee], all of these being located in the vicinity of 50 K. A search for the occurrence of a corresponding "50 K anomaly" in the magnetic susceptibility was not successful [72Jam, 78Mil]; the claim of [77Dek] to having seen such an anomaly lacks credibility. Although the anomaly was not found in measurements of the elastic moduli made in the megacycle range using ultrasonic methods [79Hsu], it did show up in modulus and internal friction measurements made with vibrating foils or torsionally oscillating wires at low frequency (320 down to ~1 hertz) [76Jac1, 76Zim]. A 50 K anomaly also appeared in the ultrasonic attenuation measured at megacycle frequencies [69Cha]. There is, so far, no clear indication of any anomalous behavior in proton nuclear magnetic resonance measurements on PdH_X in the T-X region, for the 50 K anomaly [87Avr]. Time-dependent effects were found in the resistivity [69Ho] and in the measurements of the specific heat and of spontaneous heat generated during the transition process [77Jac], the time constants for which were later shown to be closely related to the growth of the A_2B_2 superlattice reflection [83Bon]. The importance of relaxation times in the transition process indicated the need to allow for "annealing times" that were long enough for the transition to progress sufficiently in the body of the crystal for the establishment of the ordered structure to be clearly observed [79Ell] at the very low temperatures that were relevant. Subsequently, the two ordered structures were observed by [78And1] and [79Ell] (see "Crystal Structures and Lattice Parameters"). For the A_2B_2 structure found in the concentration range* ($0.63 < X < 0.69$), a superlattice reflection** (1,1/2,0) is observed, consistent with an earlier prediction [78Gol2]. For the A_4B structure ($0.75 < X < 0.8$), the corresponding point in reciprocal space is (4/5,2/5,0). Apart from the superlattice reflections, a short-range order (SRO) has been found to occur in the vicinity of the (1,1/2,0) point, at and above the observed anomaly temperature for the

*To avoid a bulky format we quote only X values in this section. However, if required, the corresponding values of at.% H can be obtained by using: at.% = $[(X/(1 + X)] \times 100$.

**This designation is for a wave vector in the reciprocal space for the fcc lattice, without the factor $2\pi/a$ being explicitly shown (a is the fcc lattice constant). Such usage is standard in treatments of superlattice reflections and neutron scattering from these crystals and is used throughout the present discussion on the ordering of the hydrogens.

whole of the range of X so far investigated ($0.63 < X < 0.78$). The form of this SRO shows a significant temperature dependence. A schematic phase diagram for the range of temperatures and concentrations involved is shown in Fig. 4, which is based on that of [82Bon], with additional information taken from [84Bla2] together with some additional experimental data (see below). The labelling of the ordered structures has been left as A_2B_2 and A_4B, rather than adopting a terminology analogous to CuAu I etc., because the ordered arrangements are of interstitial hydrogens and vacancies. A discussion of the crystal structure aspects of this region of the phase diagram for the Pd-H system is given in more detail under "Crystal Structures and Lattice Parameters." These ordered structures are of general interest because of the effects due to the mobility of the hydrogens at very low temperatures and because of the possibility of a connection between the A_4B structure and superconductivity in Pd-H at high X values [83Bal, 83Sta, 84Bal].

Measurements at low temperatures of the resistivity [72Sko] in PdH_X samples with $X = 0.81$ (44.8 at.% H) and $X = 0.87$ (46.5 at.% H) (i.e. in the composition range where the ordering processes, discussed above, occur) showed the existence of superconductivity* in these alloys, something that was not detected [72Sko, 79Sta] at compositions below 0.7 (41.2 at.% H). [72Str] measured maximum superconducting transition temperatures, T_c, of up to 9 K for samples implanted with H_{2+} ions ($X = 1$ or 50 at.% H). [72Str] also found that for PdD_X of X value equal to that for a PdH_X sample, the T_c values were ~2 K higher, in contrast to the normal isotope effect observed in superconductors described by the BCS (Bardeen, Cooper, Schrieffer) theory of superconductivity. Thus this effect came to be known as "the inverse isotope effect" (see [78Str] for a review).

[83Bal] and [84Bal] made a comprehensive study of some of the superconducting parameters of the Pd-H (also the Pd-D) system and related the results to the phase diagram. In the X range from 0.84 to 0.91 (i.e. between 45.7 and 47.6 at.% H), the results indicated the presence of two superconducting forms of PdH_X (both being type II superconductors). These findings were also consistent with the phase diagram proposed by [82Bon] for the Pd-D system (see below), the major features of which are shown in Fig. 4. However, when relating the limits of [82Bon] for a mixed-phase region presented in Fig. 4 to those given by [84Bal], it should be kept in mind that, apart from the expected differences between experimental [83Bal, 84Bal] and model predictions of the phase boundaries [82Bon], isotope shifts in phase boundary locations are also possible. Further, [83Bal] and [84Bal] pointed to the importance of specifying the history of the PdH_X (also PdD_X) sample ($X < 0.91$) during its cooling to temperatures near T_c since the relative abundance for the two phases present in the sample and the H(D) concentration of each phase will depend on this factor.

Liquid Pd

The change in the H solubility of Pd at the melting point is shown in Fig. 6, replotted from [80Kal]. Earlier attempts [10Sie, 14Sie1, 14Sie2] at measuring the H solubility of liquid Pd appeared to be seriously affected by impurities in the Pd and by interaction of the molten Pd with the crucible that contained it. [80Kal] avoided crucible problems by using electromagnetic levitation. After the experimental samples attained equilibrium, they were quenched and stored in liquid nitrogen, and subsequently extraction methods were used to determine the H concentration at the prequenching temperature. The Pd used was of 99.98 wt.% nominal purity. Figure 6 shows that the solubility of H in liquid Pd is ~2.3 times its value in the solid at the melting temperature, T_m. This is in line with evidence for the H solubility in other metals above their melting points [76Fro, 91Fuk]. [80Kal] gives no information on the depression of T_m for Pd with the addition of H, but [91Fuk] gives an estimate for all fcc H absorbing metals and comments that the amount of depression is similar to that for other interstitial solute atoms, i.e.:

$$\Delta T_m/\Delta X = -(2 \text{ to } 5) \times 10^3 \text{ K}$$

*Pure Pd is not a superconductor above 0.0017 K [78Web].

Crystal Structures and Lattice Parameters

Both the α and α′ phases** have the same fcc structure as the Pd host lattice but with lattice parameters greater than that of pure Pd. In these two phases, ND established that the octahedral interstitial sites are occupied randomly by hydrogens.*** Only at very low temperatures has an ordered arrangement of

**From XRD measurements at 333 K, [79Eve] reported the existence of two additional fcc phases for the Pd-H system, with lattice parameters between those of the α and α′ phases. No subsequent verification of this report has been published.

***We use the term hydrogen to denote a proton subject to electronic screening inside the metal, without implying anything specific about the screening, except to emphasize that we are not considering a hydrogen atom inside the metal (see [78Swi] for a review).

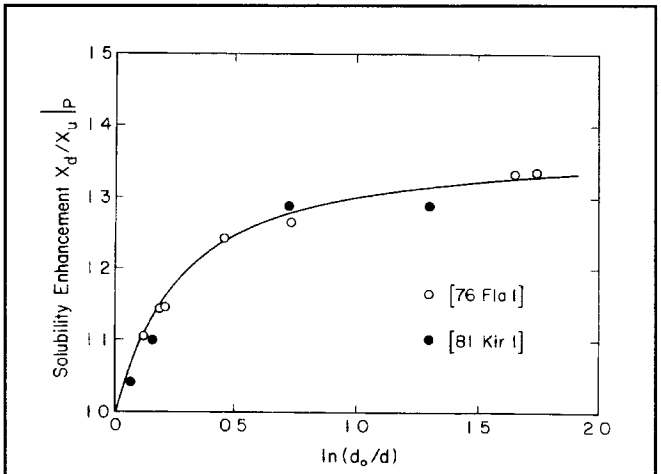

Fig. 8 Solubility enhancement at 22 °C for $X > 10^{-4}$, as a function of deformation. Deformation is expressed as the ratio of sample thickness before cold rolling (d_o) and after (d).

hydrogens been confirmed [78And1, 79Ell] (see "Low-Temperature Ordered Structures").

The value of the lattice constant for pure Pd in Table 1 was obtained by [78Kin] with a reproducibility of 1:40 000 and is lower than the values adopted by [Pearson2] (0.38907 nm), [King1] (0.38901 nm), or [Massalski2] (0.38903 nm). Apart from experimental factors [78Kin] attributed this slightly lower value at room temperature to the greater nominal purity of the specimen they used (99.993 wt.%).

From precise measurements on the single-phase region of the system (at $T = 327$ °C, $0 < X < 0.65$ or 0 to 39.4 at.% H), [86Fee1] determined the relative volume change, $\Delta V/V_o$, produced by absorption of H to a concentration X, to be:

$$\Delta V/V_o = 0.200\,X - 0.0492\,X^2 \qquad \text{(Eq 6)}$$

This is to be compared with:

$$\Delta V/V_o = 0.198\,X$$

obtained by [74Rib1] for a much wider range of temperatures and up to comparable values of X but without strict avoidance of effects due to passage of the sample through the α/α' mixed-phase region. If the X-ray lattice parameter data of [87Bal] (for Pd-H samples not taken through the mixed-phase region) are converted to the 327 °C used by [86Fee1], they give values that are much closer to the extrapolated $\Delta l/l_o$ curve of [86Fee1] than the data that [86Fee1] quote from extrapolating the results of [71Bar] and [75Sch]. Both of these latter sets of data were subject to distortions resulting from the passage of the experimental samples through the α/α' mixed-phase region.

XRD measurements made on samples of Pd-H over a wide range of H concentrations showed that the Pd-H lattice parameters were, in all cases, greater than that of the host metal [23Mck, 23Yam, 27Lin, 33Kru, 44Owe, 61Mae, 62Abe, 64Axe, 64Mae, 65Ver, 79Eve].

ND measurements by [57Wor] failed to determine, unequivocally, the location of hydrogens in the low-concentration α phase. Indirect results favoring octahedral interstitial occupancy of the fcc lattice were obtained from inelastic neutron scattering (INS) measurements [67Sko] and from ND experiments using Pd-Ag-H and Pd-Au-H alloys [68Mae]. Direct evidence of the interstitial location of the hydrogens in the pure α phase was first provided by [71Nel], who obtained the necessary H concentration for reliable ND results by increasing the H pressure to 20×10^5 Pa and elevating the temperature to 340 °C.

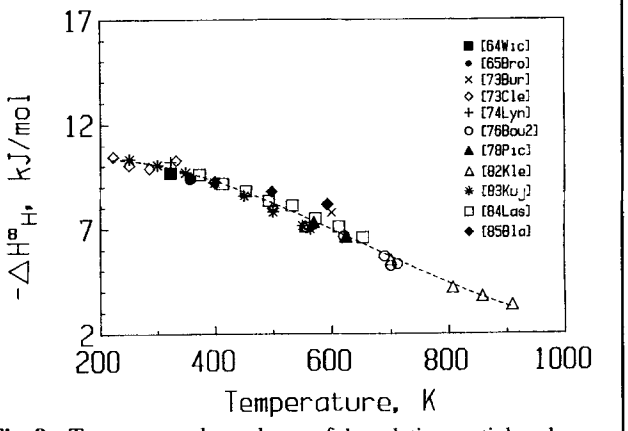

Fig. 9 Temperature dependence of the relative partial molar enthalpy of solution at infinite dilution for H in the Pd-H system.

Within the α' phase, the hydrogens occupy octahedral positions at room temperature as determined from ND measurements [57Wor, 60Ber, 65Fer, 71Nel].

Low-Temperature Ordered Structures

Evidence for the formation of an ordered phase in the vicinity of 50 K (see "Solubility") was first obtained [78And1, 78And2] using ND on single crystals of PdD_X ($X = 0.64$ and 0.67 or 39 and 40 at.% D).* The intensities of the observed (1,1/2,0) superlattice reflections were low, ~10^{-3} of the intensity of observed fcc reflections of the Pd lattice. The corresponding ordered structure is tetragonal, with space group $I4_1/amd$, which is stoichiometric at $X = 0.5$ (33.3 at.% D) and is shown as A_2B_2 in Fig. 4. Because $X = 0.5$ is in the mixed $\alpha + \alpha'$ region, the A_2B_2 structure cannot be simply observed at its stoichiometric composition. This observation of the $I4_1/amd$ structure is, so far, the only known example either in the substitutional alloy form or the interstitial/vacancy form found in Pd-D, of this frequently cited [73Kha] superlattice of the fcc system. Another ordered structure was found using ND on a single crystal of PdD_X ($X = 0.76$ or 43.2 at.% D) at a temperature of 70 K [79Ell]. The superlattice reflection, in this case, involved the (4/5,2/5,0) point in reciprocal space, corresponding to an ordered structure with the $I4/m$ space group, denoted as A_4B in Fig. 4 and which is stoichiometric at $X = 0.8$. This structure also has a tetragonal unit cell. [80Bla] confirmed this determination of the (4/5,2/5,0) superstructure reflection using a single crystal of PdD_X ($X = 0.78$ or 43.8 at.% D) at temperatures of 70 and 75 K. In all of the above investigations of ordering in Pd-D, evidence of short-range ordering (SRO) was found in the vicinity of the (1,1/2,0) point. Thus, over the range of concentrations for which neutron scattering techniques (including ND) have been used to study the "50 K anomaly" (~$0.63 < X <$ ~0.78),** the hydrogens were found to order on 420 planes in the fcc lattice of interstitials. For the A_2B_2 structure (~$0.63 < X <$ ~0.69), the ordered arrangement at full stoichiometry consists of two 420 planes of hydrogens

*Almost all the neutron diffraction and scattering measurements have been made on Pd-D because for D there is no significant problem with incoherent scattering of the neutrons. There is some isotope effect in some features of the "50 K anomaly," but from what is known so far, the ordering process occurs for both H and D, with no difference in the ordered structures having been discovered. Thus for this one situation, we present the available evidence for ordering in Pd-D because it is a far more comprehensive body of information. Much of the available information on the "50 K anomaly" has been obtained with H as well as D, and in keeping with our general usage, we use the term hydrogen to denote either isotope.

**To avoid a bulky format we quote only X values in this section. However, if required, the corresponding values of at.% H can be obtained by using: at.% = $(X/(1 + X)] \times 100$.

followed by two 420 planes of vacancies. For the A_4B structure ($\sim 0.75 < X < \sim 0.8$), the arrangement changes to one in which, at stoichiometry, the hydrogens occupy four 420 planes followed by one 420 plane of vacancies. This corresponds to the Ni_4Mo structure, with the hydrogens and the vacancies corresponding to the Ni and Mo, respectively. Order-disorder transitions in alloys have been treated within a harmonic approximation for the Gibbs energy by [68Cla] and [73Kha] and, more generally, by [75Fon], who included further developments of the concepts of special points in the Brillouin zone [42Lif]. According to these concepts, in fcc lattices with first and second nearest neighbor interactions, V_1 and V_2, such that $0 \leq V_2/V_1 \leq 0.5$, SRO should only appear at the (1,1/2,0) special point of the reciprocal lattice.

The experimental evidence for ordering in PdD_X is in accord with this prediction, in line with an earlier suggestion [78Gol2] but only for $X < 0.7$, [78And1, 78And2]. This was further supported by a Monte Carlo simulation [82Bon] of ordering in PdD_x, which assumed $V_2 = 0.25V_1$ and successfully reproduced the observed behavior for $X < 0.69$. [80San], also using $V_2 = 0.25V_1$ in a cluster variation calculation, had obtained a phase diagram with ordered regions that was in close agreement with that of [82Bon], particularly at stoichiometric concentrations, i.e. at $X = 0.5$ etc. For $X < 0.69$, the (1,1/2,0) superlattice reflection is observed to evolve out of the SRO, and the time dependence of this evolution has been used to determine a couple of transition temperatures for the ordering process (see Fig. 4). For higher X values, however, the center of the SRO distribution is displaced from the (1,1/2,0) position, and the X-dependence of this displacement has been measured [84Bla1]. Even after long "annealing times" in the transition region (e.g. ~190 h for $PdD_{0.73}$), no transition to a long-range ordered structure was observed for $\sim 0.71 < X < \sim 0.75$, whereas for larger X values, the superlattice reflections at (4/5,2/5,0) appeared after an "annealing" of just a few hours. Thus for $X > 0.7$, the [75Fon] analysis did not appear to have as much relevance [78Gol1] to the experimental observations. The observations can be reconciled in terms of the "mixed domain" model [81Bla, 84Bla1], which represents the observed SRO as being due to the presence of a mixture of micro domains of the A_nB type in which the ordering on 420 planes ranges through arrangements such as A_2B, A_3B, in addition to the observed A_2B_2 and A_4B. Locally, the unit cells of these structures can be mutually transformed by simple exchange of one or two filled and vacant sites. This possibility can be viewed as the basis for formation of a mosaic tile arrangement of unit cells of the A_nB type, and [81Bla] have shown that the observed SRO may be accounted for by neutron scattering from such a mosaic. In the range ($\sim 0.7 < X < \sim 0.75$), [81Bla] view the PdD_X system as remaining "frustrated" in the mixed domain state, but at higher concentrations, closer to the stoichiometric composition for A_4B, i.e. $X = 0.8$, long-range order indicated by the (4/5,2/5,0) superlattice reflection is established directly. This situation is summarized in the schematic phase diagram shown in Fig. 4, which is based on that of [82Bon] and [84Bla2]. When considering the location of transition points in the T-X plane, presented in Fig. 4, it should be kept in mind that the work of [81Her] showed that the location of the 50 K resistivity anomaly depended on the direction of the temperature change used to reach the anomaly temperature region and also on the rate of that temperature change. Such a hysteresis often applies to indications of transition temperatures and, in general, is seldom indicated in descriptions of these processes. No account of hysteresis has been included in Fig. 4. The T-X diagram of Fig. 4 displays the known long-range ordered phase fields and the regions in which short-range order (SRO) has been observed. The $\alpha + \alpha'/\alpha'$ and $\alpha + A_2B_2/A_2B_2$ boundaries are located according to the magnetic susceptibility measurements of [78Mil]. The A_2B_2/α' boundary is from the calculations of [82Bon]. The points shown on this boundary are from [83Bon], and the boundary is consistent with resistivity measurements of [81Her]. Locations of the SRO and mixed-domain regions are from [84Bla2], and the hashed curve gives the approximate location of the "50 K anomaly" as most extensively indicated by resistivity measurements [79Ell, 81Her]. The suggestion of mixed-phase regions adjacent to the A_4B phase field in [82Bon] has been retained, but the boundaries have been relocated. The position shown for the lower concentration $\alpha'/(\alpha' + A_4B)$ boundary is merely to indicate its existence, whereas the location of the corresponding $(\alpha' + A_4B)/A_4B$ boundary is based on the observation (for $X = 0.78$) that the intensity of the (4/5,2/5,0) reflection was 2% of the (200) Bragg reflection, indicating an almost completely ordered sample according to [84Bla1]. The other point on this boundary is from [79Ell]. Also, the requirement for the presence of the mixed-phase regions is indicated by the observation [80Bla] that the transition to the A_4B state is first order (nucleation mechanism). The conformity of the observed structures for the ordered phases (i.e. A_2B_2 and A_4B) with the Landau-Lifshitz rules for ordering transitions [80Lan], has been comprehensively treated by [75Fon].

These transformations in PdD_X are rather unique in that they take place with no measurable distortion of the Pd unit cell [75Mue, 76Hun, 78Kin], although the superlattices formed do not themselves have cubic symmetry. So far, there is no clear indication from theoretical modelling of the form of the PdD_X (PdH_x) phase diagram for $X > 0.7$, and the only experimental indications come from two ND results [79Ell, 80Bla] and some inferences from superconductivity measurements [83Bal, 83Sta, 84Bal]. [91Ros] examined the time/temperature dependence of the evolution of the (1,1/2,0) superlattice reflection and concluded that they could account for the time dependence by assuming that it was caused by strain energy built up as the tetragonal symmetry of the superlattice is imposed on the cubic symmetry of the disordered state. Under these strain limiting conditions, [91Ros] estimated that for a sample of $PdD_{0.64}$ at 55 K, the limiting value (i.e. at infinite "annealing time") of the average length of one of the antiphase boundaries formed was 13.4 nm. From this study of the growth in size of antiphase boundaries, it seems that the transition to the ordered A_2B_2 state conforms to a number of the features of a higher order* transition. Although critical point exponents for this transition have been published [81Bon, 83Bon,

*The term "second order transition" used by [91Ros] and others in the present context should preferably be replaced by the more generally valid term: "higher order transition" [57Pip].

91Ros], no clear assignment of how they relate to a model for the transition process has yet been made.

α′ Phase

The lattice parameter of the α′ phase increases linearly with H absorption up to at least $X = \sim 0.9$, as determined by [87Bal], who obtained a set of $a(X)$ data, at 77 K (–196 °C), which were unaffected by the lattice damage due to the passage of the PdH_X sample through the $\alpha + \alpha'$, mixed-phase region and were thus more simply related to the dilation produced by the introduction of H into the Pd lattice (see below). There are no equivalent data for room temperature, but the [87Bal] data may be roughly converted to room temperature by adding the amount of $\delta = 0.0009$ nm, determined by [75Sch] from their α′ samples, to the $a(X)$ relation quoted by [87Bal], to give:

$$a = 0.39534 + 0.01234X \text{ nm} \quad \text{(Eq 7)}$$

for lattice parameters in the range $0.7 < X < 0.9$ at room temperature. From Eq 7, the room temperature lattice parameter at $X = 1$ (50 at.% H) extrapolates to 0.4077 nm. It must be emphasized, when comparing this value with other estimates for $X = 1$, that this estimate is for measurements that are free from the distortion effects of the α/α′ transition. If the [87Bal] measurements, which do include the effects of the α/α′ transition are used, the $X = 1$ value for a is 0.4088 nm at 77 K and 0.4097 nm at room temperature. These are to be compared with values of 0.4090 nm and 0.4099 nm, respectively, for these temperatures [75Sch], which were also affected by the distortions produced by the α/α′ transition.

From XRD studies of the diffraction effects accompanying the decomposition of the α′ phase, [78Kin] found that, whereas the α′ phase profiles were well resolved, the α phase reflections showed considerable strain broadening. These observations, together with earlier findings of broadened electron diffraction spots by [76Jam], led [78Kin] to attribute the line broadening in the α phase to the effect of the high dislocation density generated by the α/α′ transformation, as opposed to an early explanation of finely dispersed crystallites (see [66Mae] for a review). A contribution of extended defects to XRD line broadening, as developed by [69Kri], is also consistent with this explanation.

[87Bal] used XRD to study α′ phase samples in the range $0.70 < X < 0.92$ or 41.2 to 47.9 at.% H. They found that the lattice parameter at any given H concentration and temperature differed depending on whether the sample history had taken the sample through the mixed-phase α/α′ region or had avoided it. Least-squares fits to the two groups of measurements provided:

$$a = 0.39380 + 0.01498\,X \text{ nm} \quad \text{(Eq 8)}$$

for samples taken through the mixed-phase region, and

$$a = 0.39534 + 0.01234\,X \text{ nm} \quad \text{(Eq 9)}$$

in the case of samples for which the mixed-phase region was avoided.

[87Bal] inferred from previous experience (see [79Ho]) and the developments of Krivoglaz and coworkers (e.g. [81Bar]), that the lattice parameter changes are due to internal stresses resulting from the progression of the α/α′ transformation as the PdH alloys is moved through the mixed-phase region. Therefore, when determining H concentration from lattice parameter measurements (as in [75Sch]), the path used should avoid mixed-phase regions. Results of room temperature measurements [88Nyg] of the density of single crystals of PdH_x, which were prepared by avoiding the mixed-phase region are in accord with the ideas developed by [87Bal]. for $0.64 < X < 0.76$ (39 to 43.2 at.% H), the density was fitted to the straight line:

$$\rho = 11.921 - 1.681\,X$$

where ρ is in $kg/m^3 \times 10^3$

Tetragonal $PdH_{1.33}$

[80Sem] reported identification of a tetragonal structure for PdH_X with $X = 1.33$, found in thin films (thickness 50 to 100 nm) produced either by loading from the gas phase or by means of H ion bombardment. The lattice parameters were determined to be: $a = 0.2896$ and $c = 0.3330$ nm. [80Sem] suggest that the H are in an ordered arrangement on tetrahedral sites in a body-centered tetragonal lattice and that the metal lattice displays the unusual feature of having a large number of metal atom vacancies. [80Sem] provide no direct information on the H locations, but they do claim to find agreement between the amount of H retained in the Pd lattice, determined by vacuum extraction, and the number of H sites they assign from fitting of their electron diffraction data. No confirmation of this tetragonal structure has been reported so far, and therefore, it has not been included in Table 1.

Theoretical Calculation of Lattice Parameter Values

From a calculation of the total energy for stoichiometric PdH, [91Pap] examined its variation with respect to possible lattice parameter values and obtained an equilibrium value of lattice parameter that was within 0.3% of the experimental value of 0.4068 nm obtained from an extrapolation of Eq 9 to $X = 1$. This extrapolation gives the closest available estimate of the lattice parameter, for PdH, at 0 K and one which is free from the distortions due to the α/α′ transition. It is also an improvement on the comparison with experiment made by [91Pap]. The results from these calculations were obtained using the now standard concepts of the electronic structure of Pd-H [78Swi] without the need of any assumptions [89Jon] involving additional forms of excitation in the Pd-H crystal.

Thermodynamics

Since the first calorimetric measurement of the absorption enthalpy of H in Pd [1873Fav], the thermodynamic properties of this system have been extensively investigated.

The temperature dependencies of the relative partial molar enthalpy $\Delta H_H = H_H - \frac{1}{2} H^0_{H_2}$) and of the relative partial molar entropy $\Delta S_H = S_H - \frac{1}{2} S^0_{H_2}$ for H absorption in Pd at infinite dilution ($X \rightarrow 0$) i.e. of ΔH^{∞}_H and ΔS^{∞}_H, were directly determined at very low X values using an isochoric absorption method [73Cle]. Figures 9 and 10 show these values in the temperature range 200 to 500 K for $5 \times 10^{-4} < X < 5 \times 10^{-3}$ (5×10^{-2} to 5×10^{-1} at.% H), as well as those obtained from equilibrium isotherm measurements, at higher X values [64Wic, 65Bro,

73Bur, 83Kuj, 84Las] and from calorimetric measurements [74Lyn, 76Bou2, 78Pic, 82Kle]. Figures 9 and 10 show that ΔH_H^{∞} and ΔS_H^{∞} become less negative with increasing temperature and that there is good agreement between the values of the different studies. By fitting these data (all with equal weight) to polynomials in T, the temperature dependencies of ΔH_H^{∞} and of ΔS_H^{∞} (dashed curves in Fig. 9 and 10, respectively) have been fitted by the relations:

$$\Delta H_H^{\infty} = -9.20 - 1.29 \times 10^{-2}\, T + 3.97 \times 10^{-5}\, T^2 - 2.02 \times 10^{-8}\, T^3 \quad \text{(Eq 10)}$$

in J/K0.5 mol H_2 and

$$\Delta S_H^{\infty} = -71.78 + 7.02 \times 10^{-2}\, T - 6.88 \times 10^{-5}\, T^2 + 2.89 \times 10^{-8}\, T^3 \quad \text{(Eq 11)}$$

in kJ/0.5 mol H_2. Both equations are valid for $200 < T < 1000$ K.

Recently, [86Las] calculated ΔH_H^{∞} and ΔS_H^{∞} (also ΔG_H^{∞}) for H and its isotopes D and T as continuous functions of temperature from 0 to 1500 K. [86Las] used an expression for the partition function of H dissolved in Pd that was resolved into the ground-state energy and the sum over the thermally populated energy states. Their data on the equilibrium constant, K_H^{∞}, for the absorption of H in Pd, which was in good general agreement with other data in the literature but much more extensive, was used to determine the five assignable parameters in the partition function relation. These [86Las] calculated values of ΔH_H^{∞} and ΔS_H^{∞} have a minimum (in the vicinity of 200 K) corresponding to the region of temperature where, according to the analysis of [86Las], the thermal population of vibrational states of H in Pd becomes important. This predicted minimum is just below the temperature range of presently available experimental data for ΔH_H^{∞} and ΔS_H^{∞}.

A variation of ΔH_H with X has been reported [73Bur, 76Bou1, 76Bou2, 78Far, 78Lab, 81Wic, 85Wic, 86Fee1]. As recommended values, Fig. 11 shows those reported by [85Wic] from equilibrium measurements on desorption isotherms, all from the same laboratory and having the widest range of X values in the same group of measurements. The majority of the data

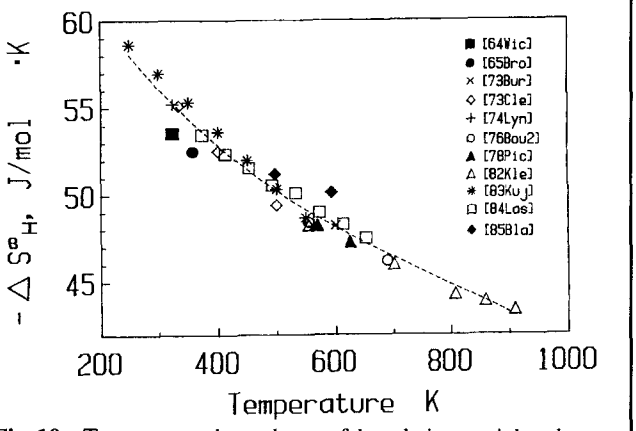

Fig. 10 Temperature dependence of the relative partial molar enthalpy of solution at infinite dilution for H in the Pd-H system.

points in Fig. 11 are derived from measurements made above the critical point temperature for the Pd-H system (T_c = 566 K), and all measurements were made outside the α/α′ coexistence region, so that the data are unaffected by the α/α′ transformation. A polynomial fit to the data points of Fig. 11 gives:

$$-\Delta H_H = 9049 + 15.31\, X + 100.9\, X^2 - 142.3\, X^3 \quad \text{(Eq 12)}$$

for $0 \le X \le 0.66$. A fit by [86Fee1] to their $-\Delta H_H$ data obtained from isotherm measurements also made above the critical point temperature, for $0 \le X \le 0.4$, is in fairly close agreement with that of Eq 12. The experimental data of Fig. 11 show a maximum in $|\Delta H_H|$ located near $X = 0.5$. Similar behavior for $|\Delta H_H|$ had been reported earlier [76Eva, 83Kuj]. This maximum and the subsequent decline in $|\Delta H_H|$ values above $X \cong 0.55$ is consistent with the form of the chemical potential for the Pd-H system [83Kuj]. Calorimetric measurements at 298 K [91Fla] show this decline of $|\Delta H_H|$ with X in the pure α′ region very clearly.

Along with the X dependence of $|\Delta H_H|$, the X dependence of the quantity ΔS^{ex}, the relative partial excess entropy, has often been reported [78Pic, 83Kuj, 85Wic] where this quantity is usually defined by:

$$\Delta S^{ex} = \Delta S_H - S_{conf}$$

in which S_{conf} is the ideal configurational entropy and ΔS_H is the relative partial entropy used above. Published estimates of the ideal configurational entropy are usually based on assuming the ideal solution model, so ΔS^{ex} is specialized* in the sense that a dilute solution approximation applies, including no H-H interaction in the metal-hydrogen lattice. Attempts at simple modifications of these assumptions have been made (see [72Fla] for a review). We do not report on the X variation of ΔS^{ex}. We have reported only on ΔS_H, which is obtained directly from observable processes without special assumptions. As the principal use for ΔS^{ex} has been to draw inferences concerning the microscopic characteristics of an M-H system, its omission is consistent with providing information that is primarily focused on the phase diagram related features of the Pd-H system. For similar reasons, we have not reported on developments such as those by [84Gri] concerning relationships between microscopic parameters of the electronic band structure of an M-H system, such as Pd-H, and the partial enthalpy ΔH_H.

Up to the present time, attempts to derive microscopic properties for M-H alloys from macroscopic thermodynamic measurements, principally through estimates of the partial excess entropy, have lacked the precision and the detail that is available from inelastic neutron scattering measurements on single crystals of these alloys. The specifics of H site occupancy, including relative site occupancy, as well as site characteristics, including details of the potential well configuration on a site and the vibrational spectrum for the interstitial H are all attainable, with useful precision, from such neutron scattering meas-

*The literature concerning "excess entropy" reveals some variation in the way this quantity is designated. Treated as a differential ΔS^{ex}, i.e. the relative, partial excess molar entropy [73Cle], either a positive or negative sign is permitted, but treated as the thermodynamic variable, S, [83Kuj, 85Wic, 91Fla], only a positive sign is appropriate [80Lan].

urements. Several commentaries, pointing out the greater utility and reliability of the information obtained from inelastic neutron scattering, compared with that obtained from macroscopic thermodynamics, have been published [77Mag, 78Rus, 91Hem].

The enthalpy and entropy of transformation from the α to α′ phase ($\Delta H_{\alpha\rightarrow\alpha'}$, $\Delta S_{\alpha\rightarrow\alpha'}$, and vice versa) have been most often obtained from plots of the equilibrium pressure in the two-phase (α + α′) region against $1/T$. The slope of the straight lines thus obtained represents $\Delta H_{\alpha\rightarrow\alpha'}$, and $\Delta S_{\alpha\rightarrow\alpha'}$ is obtained from the ordinate intercept of such van't Hoff plots.

Recently, calorimetrically determined values of ΔH_H became available [91Fla] that are very close to those determined from van't Hoff plots (Table 4). Values of ΔS_H were determined from the calorimetric ΔH_H values, using:

$$\Delta S_H = (\Delta H_H)_{cal}/T - 1/2(R\ln P_{eq}) \qquad \text{(Eq 13)}$$

where $P_{eq} = (P_f P_d)^{1/2}$ and P_f and P_d are the H pressures for the formation and decomposition branches of the $P(X)$ curve for a given T, through the coexistence region. The agreement between the calorimetric [91Fla] and the van't Hoff [83Las] values for ΔS_H is sufficiently good to indicate that the use of P_{eq} in Eq 13 is the correct choice, i.e. that neither P_f nor P_d can be taken to be the equilibrium value for a plateau pressure. This is consistent with the work of [79Ho] and [80Fla], which showed that both the growth of α′ in α and α in α′ are accompanied by stress (see "Equilibrium Diagram").

It has been pointed out by [82Fla] and [88Fla] that the average of the enthalpies determined from van't Hoff plots for the $\alpha \rightarrow \alpha'$ and $\alpha' \rightarrow \alpha$ transitions should agree with the calorimetric value, which the measurements of [91Fla] show to be independent of the direction of the transition to within their probable experimental error of 0.1 kJ/0.5 mol H_2. This agreement between van't Hoff and calorimetric values should hold provided that contributions from the phase boundary differences caused by hysteresis can be neglected, which the measurements of [91Fla] show to be clearly the case. The calorimetric results of [91Fla] together with the van't Hoff measurements of [83Las] distinguish clearly between the presence of a difference between $|\Delta H_H|$ values for formation and decomposition in the case of the van't Hoff measurements and the absence of such a difference in the case of the calorimetric measurements, as predicted by [82Fla]. The precision of the calorimetric values for $|\Delta H_H|$ was sufficient to demonstrate, in absolute terms, the absence of a contribution from hysteresis based energy dissipation [89Fla, 91Fla]. The values of ΔS_H obtained from the van't Hoff plots [83Las] are free of hysteresis effects and agree closely with the calorimetric ΔS_H also, further supporting the choice of $P_{eq} = (P_f P_d)^{1/2}$ as giving the relevant plateau pressure. In addition, the thermodynamic data from these two types of measurement on Pd-H and Pd-D show clearly that there is no support for any heat production in the Pd-D system [89Fle, 89Jon] beyond that available from the α/α′ transformation, for the range $0 \leq X \leq 0.77$.

[75Fla2] and [78Rud] examined the reasons why experimental values of ΔH_H and ΔS_H appeared, as reported, to be independent of temperature. Both [75Fla2] and [78Rud] obtained a term, which may be written as:

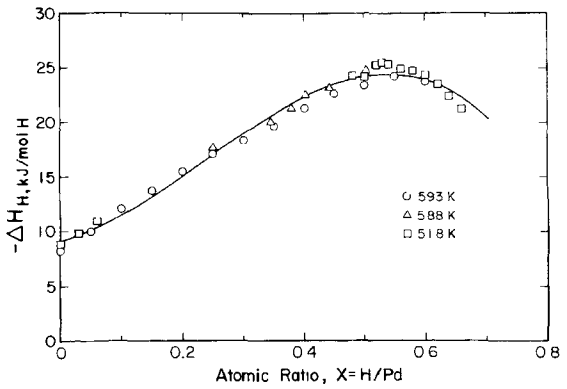

Fig. 11 Concentration dependence of the relative partial molar enthalpy for H in the Pd-H system. Data taken from [85Wic].

$$T^2\left[\frac{\partial \mu_H/T}{\partial X}\right] \cdot dX/dT$$

where μ_H is the chemical potential of the H. Both [75Fla2] and [78Rud] added this term to the relative partial molar enthalpy in making allowance for the effect of variations in X on the partial enthalpy. While [75Fla2] calculated the effect of this additional term in relation to $|\Delta H_H|$, a clear test of taking the additional term into account has not yet been made. An examination of the contribution of the additional term using the precision of the [91Fla] calorimetric results now appears to be possible. [91Fla] found that calorimetrically determined values for ΔH_H increased as the temperature was reduced below 269 K, e.g. at 249 K, $\Delta H^f_H = -20.2 + 0.23$ kJ/0.5 mol H_2 and at 195 K, $\Delta H^f_H = -23.2 + 0.64$ kJ/0.5 mol H_2.

Specific heat measurements of Pd-H at low concentrations were first reported by [56Eic], and later by [57Nac] and [63Mit] for a wide range of concentrations. Particular attention was paid by [63Mit] to the specific heat anomaly found at temperatures in the vicinity of 50 K (for alloys with $0.125 \leq X \leq 0.75$, i.e. from 11.1 to 42.9 at.% H).

Motivated by the findings of previous work performed in the same laboratory (electrical resistance [69Ho], Hall effect [71Zep], internal friction [76Jac1] on the so-called "50 K transition," [77Jac] reinvestigated this specific heat anomaly and found that the magnitude of the anomaly depended on the rate of temperature change used in the specific heat measurements. The slower the rate, the larger the anomaly [77Jac] (see "Low-Temperature Ordered Phases"). This observation showed the futility of attempts to analyze the thermodynamics of the "50 K transition" by making use of a determination of the area under the specific heat curve [72Bro, 74Sta, 76Jac3, 77Bou, 78Wic].

Other measurements of the specific heat in the low-temperature range from 1.2 to 4.2 K were reported [66Mac1, 66Mac2, 74Mac, 76Mac, 76Miz, 77Miz].

Measurements of the specific heat (at constant H concentration) through the critical-point region were reported by [74Rib2]. The principal result was that the heat capacity displayed a simple discontinuity at the critical point, consistent

with a conformity to mean field behavior for the Pd-H system (see "Equilibrium Diagram").

Cited References

1866Gra: T. Graham, "On the Absorption and Dialytic Separation of Gases by Colloid Septa," *Philos. Trans. R. Soc. (London), 156*, 399-439 (1866). (Equi Diagram; Experimental)

1873Fav: P.A. Favre, "Thermical Investigations on the Condensation of Gases into Solids," *Compt. Rend., 77*, 649-656 (1873) in French. (Thermo; Experimental)

10Sie: A. Sieverts and W. Krumbhaar, "The Solubility of Gases in Metals and Alloys," *Ber. Deut. Chem. Gesellsch., 43*, 893-900 (1910) in German. (Equi Diagram; Experimental)

14Sie1: A. Sieverts, "Palladium and Hydrogen I." *Z. Phys. Chem., 88*, 103-127 (1914) in German. (Equi Diagram; Experimental)

14Sie2: A. Sieverts, "Palladium and Hydrogen II.," *Z. Phys. Chem., 88*, 451-478 (1914) in German. (Equi Diagram; Experimental)

15Lan: I. Langmuir, "The Dissociation of Hydrogen into Atoms," *J. Am. Chem. Soc., 37*, 417-458 (1915). (Equi Diagram, Thermo; Experimental)

23Mck: L.W. McKeenan, "The Crystal Structures of the System Palladium-Hydrogen," *Phys. Rev., 21*, 334-342 (1923). (Crys Structure; Experimental)

23Yam: M. Yamada, "On the Occlusion of Hydrogen in Palladium," *Philos. Mag., 45*, 241-243 (1923). (Crys Structure; Experimental)

27Lin: J.O. Linde and G. Borelius, "Roentgen Ray and Electrical Studies of the System Palladium-Hydrogen," *Ann. Phys., 84*, 747 (1927) in German. (Crys Structure; Experimental)

29Sie: A. Sieverts, "Absorption of Gases by Metals," *Z. Metallkd., 21*, 37-51 (1929). (Equi Diagram, Crys Structure; Experimental)

33Bru: H. Bruning and A. Sieverts, "The Electrical Resistance of Palladium Wire Charged with Hydrogen Between 160 and 310 °C," *Z. Phys. Chem., 163*, 409-441 (1933) in German. (Equi Diagram, Crys Structure; Experimental; #)

33Kru: F. Kruger and G. Gehm, "Change of Lattice Constants and the Conductivity of Palladium Charged Electrolytically with Hydrogen," *Ann. Phys., 16*, 174 (1933). (Crys Structure; Experimental)

36Gil: L.J Gillespie and L.S. Galstaun, "The Palladium-Hydrogen Equilibrium and New Palladium Hydrides," *J. Am. Chem. Soc., 58*, 2565-2573 (1936). (Equi Diagram; Experimental; #)

37Lac1: J.R. Lacher, "A Theoretical Formula for the Solubility of Hydrogen in Palladium," *Proc. R. Soc. (London) A, 161*, 525-545 (1937). (Equi Diagram; Theory; #)

37Lac2: J.R. Lacher, "Statistics of Hydrogen-Palladium System," *Cambridge Phil. Soc. Proc., 33*, 518-523 (1937). (Equi Diagram; Theory)

42Lif: E.M. Lifshitz, "On the Theory of Phase Transitions of the Second Order," I, *J. Phys. U.S.S.R., 6*, 61-74 (1942); and II, *J. Phys. U.S.S.R., 6*, 251-263 (1942). (Crys Structure; Theory)

44Owe: E.A. Owen and E.St. Williams, "X-Ray Study of the Hysteresis Effect Observed in the Palladium-Hydrogen System," *Proc. Phys. Soc. (London), 56*, 52-63 (1944). (Crys Structure; Experimental)

50Wri: P. Wright, "The Effect of Occluded Hydrogen on the Electrical Resistance of Palladium," *Proc. Phys. Soc. (London) A, 63*, 727-739 (1950). (Equi Diagram; Experimental)

52Nor: R.E. Norberg, "Nuclear Magnetic Resonance of Hydrogen Absorbed into Palladium Wires," *Phys. Rev., 86*, 745-752 (1952). (Equi Diagram, Thermo; Experimental)

52Per: P.C. Perminov, A.A. Orlov, and A.N. Frumkin, "The Influence of Pressure on the Solubility of Molecular Hydrogen in the Beta Phase of the System Palladium-Hydrogen," *Dokl. Akad. Nauk SSSR, 84*, 749-752 (1952) in Russian. (Equi Diagram; Experimental)

56Eic: W. Eichenauer and L. Schaefer, "Measurements of the Specific Heat of Pure Palladium and Palladium Charged with Hydrogen," *Z. Naturforsch. A, 11*, 955-956 (1956) in German. (Thermo; Experimental)

56Lou: N. Louat, "The Effect of Temperature on Cottrell Atmospheres," *Proc. Phys. Soc. (London) B, 69*, 459-467 (1956). (Equi Diagram, Thermo; Theory)

57Nac: D.M. Nace and J.G. Aston, "Palladium Hydride. II. The Entropy of Pd2D at 0 K," *J. Am. Chem. Soc., 79*, 3623-3626 (1957). (Equi Diagram, Thermo; Experimental)

57Pip: A.B. Pippard, *Elements of Classical Thermodynamics*, Cambridge University Press, London (1957). (Crys Structure, Thermo; Review)

57Wor: J.E. Worsham, Jr., M.K. Wilkinson, and C.G. Shull, "Neutron-Diffraction Observations on the Palladium-Hydrogen and Palladium-Deuterium Systems," *J. Phys. Chem. Solids, 3*, 303-310 (1957). (Crys Structure; Experimental)

58Bes: D.N. Beshers, "On the Distribution of Impurity Atoms in the Stress Field of a Dislocation," *Acta Metall., 6*, 521-523 (1958). (Equi Diagram, Thermo; Theory)

60Ber: H. Bergsma and J.A. Goedkoop, "Thermal Motion in Palladium Hydride Studied by Means of Elastic Scattering of Neutrons," *Physica, 26*, 744-750 (1960). (Crys Structure; Experimental)

60Eve: D.H. Everett and P. Nordon, "Hysteresis in the Palladium + Hydrogen System, *Proc. R. Soc. (London) A, 259*, 341-360 (1960). (Equi Diagram; Theory)

60Hil: T.L. Hill, *Introduction to Statistical Thermodynamics*, Ch. 14, Addison-Wesley, New York (1960). (Equi Diagram; Review)

60Lev: P.L. Levine and K.E. Weale, "The Palladium + Hydrogen Equilibrium at High Pressures and Temperatures," *Trans. Faraday Soc. (London), 56*, 357-362 (1960). (Equi Diagram; Experimental; #)

60Sch: A.I. Schindler, R.J. Smith, and E.W. Kammer, "Low Temperature Dependence of the Electrical Resistivity and Thermoelectric Power of Palladium and Palladium-Nickel Alloys Containing Absorbed Hydrogen," *Proc. 10th Int. Congress Refrigeration*, Pergamon Press, New York, 74-79 (1960). (Equi Diagram; Experimental)

61Mae: A.J. Maeland and T.R.P. Gibb, "X-Ray Diffraction Observations of the Pd-H System Through the Critical Region," *J. Phys. Chem., 65*, 1270-1272 (1961). (Crys Structure; Experimental; #)

62Abe: P.C. Aben and W.G. Burgers, "Surface Structure and Electrochemical Potential of Palladium While Absorbing Hydrogen in Aqueous Solution," *Trans. Faraday Soc., 58*, 1989-1992 (1962). (Equi Diagram; Experimental)

62Bon: G.C. Bond, "The Reaction of Hydrogen at Metal Surfaces," *Catalysis by Metals*, Academic Press, London, 149-181 (1962). (Equi Diagram; Review)

62Cah1: J.W. Cahn, "Coherent Fluctuations and Nucleation in Isotropic Solids," *Acta Metall., 10*, 907-913 (1962). (Equi Diagram, Thermo; Theory)

62Cah2: J.W. Cahn, "On Spinodal Decomposition in Cubic Crystals," *Acta Metall., 10*, 179-183 (1962). (Equi Diagram, Thermo; Theory)

63Mit: P. Mitacek and J.G. Aston, "The Thermodynamic Properties of Pure Palladium and its Alloys with Hydrogen Between 30 and 300 K," *J. Am. Chem. Soc., 85*, 137-141 (1963). (Equi Diagram, Thermo; Experimental)

63Sch: N.A. Scholtus and W.K. Hall, "Hysteresis in the Palladium-Hydrogen System," *J. Chem. Phys., 39*, 868-870 (1963). (Equi Diagram; Theory)

64Axe: S.D. Axelrod and A.C. Makrides, "X-Ray Studies of Hydrogen-Silver-Palladium Electrodes," *J. Phys. Chem., 68*, 2154-2159 (1964). (Equi Diagram, Crys Structure; Experimental)

64Mae: A. Maeland and T.B. Flanagan, "Lattice Constants and Thermodynamic Parameters of the Hydrogen-Platinum-Palladium and Deuterium-Platinum-Palladium Systems," *J. Phys. Chem., 68*, 1419-1426 (1964). (Equi Diagram, Crys Structure, Thermo; Experimental)

64Wic: E. Wicke and G.H. Nernst, "Phase Diagram and Thermodynamic Behaviour of the Palladium-Hydrogen and of the Palladium-Deuterium Systems at Normal Temperature; H/D Separation Effect,"

Ber. Bunsenges. Phys. Chem., *68*, 224-235 (1964) in German. (Equi Diagram, Thermo; Experimental)

65Bro: H. Brodowsky and E. Poeschel, "Hydrogen in Palladium-Silver Alloys," *Z. Phys. Chem., Neue Folge*, *44*, 143-159 (1965) in German. (Thermo; Experimental)

65Fer: G.A. Ferguson, Jr., A.I. Schindler, T. Tanaka, and T. Morita, "Neutron Diffraction Study of Temperature-Dependent Properties of Palladium Containing Absorbed Hydrogen," *Phys. Rev.*, *137*, 483-487 (1965). (Crys Structure; Experimental)

65Sim: J.W. Simons and T.B. Flanagan, "Absorption Isotherms of Hydrogen in the Alpha-Phase of the Hydrogen-Palladium System," *J. Phys. Chem.*, *69*(10), 3773-3781 (1965). (Equi Diagram; Experimental)

65Ver: Zh.L. Vert, I.A. Mosevich, and I.P. Tverdovskii, "X-Ray Study of the Solubility of Hydrogen in Finely Divided and in Massive Palladium," *Russ. J. Phys. Chem.*, *39*, 566-568 (1965). (Crys Structure; Experimental)

66Mac1: C.A. Mackliet and A.I. Schindler, "Low-Temperature Specific Heat of Palladium Containing Interstitial Hydrogen," *Phys. Rev.*, *146*(2), 463-467 (1966). (Thermo; Experimental)

66Mac2: C.A. Mackliet and A.I. Schindler, "Exothermic Process in H-Pd Alloys in the 1.2-4.2 K Range," *J. Chem. Phys.*, *45*, 1363-1365 (1966). (Thermo; Experimental)

66Mae: A. Maeland and T.B. Flanagan, "The Hydrogen-Palladium System: The Role of X-Ray and Neutron Diffraction Studies," *Platinum Met. Rev.*, *10*(1), 20-23 (1966). (Crys Structure; Review)

67Aro: R.R. Arons, J. Bouman, M. Wijzenbeek, P.T.A. Klaase, C. Tuyn, G. Leferink, and G. De Vries, "Internal Friction of Palladium Containing Hydrogen," *Acta Metall.*, *15*, 144-147 (1967). (Equi Diagram; Experimental)

67Fio: N.F. Fiore and C.L. Bauer, "Binding of Solute Atoms to Dislocations," *Prog. Mater. Sci.*, *13*, 87-134 (1967). (Equi Diagram, Thermo; Theory)

67Lew: F.A. Lewis, *The Palladium Hydrogen System*, Academic Press, London, New York (1967). (Equi Diagram; Review)

67Sko: K. Skold and G. Nelin, "Diffusion of Hydrogen in the alpha-Phase of Pd-H Studied by Small Energy Transfer Neutron Scattering," *J. Phys. Chem. Solids*, *28*, 2369-2380 (1967). (Crys Structure, Thermo; Experimental)

68Abe: P.C. Aben, "Palladium Areas in Supported Catalysts," *J. Catal.*, *10*, 224-229 (1968). (Equi Diagram, Thermo; Experimental)

68Cla: P.C. Clapp and S.C. Moss, "Correlation Functions of Disordered Binary Alloys II," *Phys. Rev.*, *171*, 754-763 (1968). (Crys Structure; Theory)

68Hay: C.T. Haywood and L. Verdini, "Electrical Resistivity Measurements in Palladium-Hydrogen Alloys," *Can. J. Phys.*, *46*, 2065-2071 (1968). (Equi Diagram; Experimental)

68Ho: N.S. Ho and F.D. Manchester, "The Electrical Resistivity of Palladium-Hydrogen and Palladium-Deuterium Alloys Between 4 and 300 K," *Can. J. Phys.*, *46*, 1341-1345 (1968). (Equi Diagram; Experimental)

68Mae: A.F. Maeland, "A Neutron-Diffraction Study of the alpha Phase in the Palladium-Gold-Hydrogen and Palladium-Gold-Deuterium Systems," *Can. J. Phys.*, *46*, 121-124 (1968). (Crys Structure; Experimental)

68Sko: T. Skoskiewicz and B. Baranowski, "Investigation of the Electrical Resistance Anomaly in the Palladium-Hydrogen System," *Phys. Status Solidi*, *30*, K33-K35 (1968). (Equi Diagram; Experimental)

69Ale: G. Alefeld, "Hydrogen in Metals as an Example of a Lattice Gas with Phase Transitions," *Phys. Status Solidi*, *32*, 67-80 (1969). (Equi Diagram; Theory; #)

69Bar: B. Baranowski and R. Wisniewski, "The Electrical Resistance of Palladium-Gold Alloy (50 wt.% Au and Pd) in Gaseous Hydrogen up to 24000 Atmos. at 25 °C," *Phys. Status. Solidi*, *35*, 593-597 (1969). (Equi Diagram; Experimental)

69Cha: K.C. Chan, "Ultrasonic Propagation in Some Palladium-Hydrogen Alloys," MSc thesis, University of Toronto, Chapter III (1969). (Equi Diagram; Experimental)

69Ho: N.S. Ho and F.D. Manchester, Time-Dependent Effects Associated with the 50 K Resistivity Anomaly in the Pd-H and Pd-D Systems," *J. Chem. Phys.*, *51*, 5437-5439 (1969). (Equi Diagram, Thermo; Experimental)

69Kri: M.A. Krivoglaz, "Theory of X-Ray and Thermal-Neutron Scattering by Real Crystals," Translation from Russian, S.C. Moss, Ed., Plenum Press, New York, Ch. IV (1969). (Crys Structure; Theory)

71Bar: B. Baranowski, S. Majchrzak, and T.B. Flanagan, "The Volume Increase of fcc Metals and Alloys due to Interstitial Hydrogen over a Wide Range of Hydrogen Contents," *J. Phys. F, Met. Phys.*, *1*, 258-261 (1971). (Crys Structure; Experimental)

71Nel: G. Nelin, "A Neutron Diffraction Study of Palladium Hydride," *Phys. Status Solidi (b)*, *45*, 527-536 (1971). (Crys Structure; Experimental)

71Wis: R. Wisniewski and A.J. Rostocki, "Hall Effect in the Pd-H System," *Phys. Rev. B*, *3*, 251-252 (1971). (Equi Diagram; Experimental)

71Zep: S. Zepeda and F.D. Manchester, "The Hall Coefficient of Pd and Some beta-Phase PdH Alloys," *J. Low Temp. Phys.*, *4*, 127-134 (1971). (Equi Diagram, Thermo; Experimental)

72Ale: G. Alefeld, "Phase Transitions of Hydrogen in Metals due to Elastic Interaction," *Ber. Bunsenges. Phys. Chem.*, *76*, 746-755 (1972). (Equi Diagram; Theory)

72Bro: H. Brodowsky, "On the Non-Ideal Solution Behavior of Hydrogen in Metals," *Ber. Bunsenges. Phys. Chem.*, *76*, 740-746 (1972). (Thermo; Experimental)

72Buc: H. Buck and G. Alefeld, "Hydrogen in Palladium-Silver in the Neighborhood of the Critical Point," *Phys. Status. Solidi (b)*, *49*, 317-327 (1972). (Equi Diagram; Experimental)

72Eer: E.P. Eer Nisse, "Simultaneous Thin-Film Stress and Mass-Change Measurements Using Quartz Resonators," *J. Appl. Phys.*, *43*, 1330-1337 (1972). (Equi Diagram; Experimental)

72Fla: T.B. Flanagan and W.A. Oates, "Thermodynamics of Metal/Hydrogen Systems," *Ber. Bunsenges. Phys. Chem.*, *76*, 706-714 (1972). (Thermo; Experimental)

72Jam: H.C. Jamieson and F.D. Manchester, "The Magnetic Susceptibility of Pd, PdH and PdD between 4 and 300 K," *J. Phys. F, Met. Phys.*, *2*, 323-336 (1972). (Equi Diagram; Experimental)

72Sko: T. Skoskiewicz, "Superconductivity in the Palladium Hydrogen and Palladium-Nickel-Hydrogen Systems," *Phys. Status Solidi(a)*, *11*, K123-K126 (1972). (Equi Diagram; Experimental)

72Str: B. Stritzker and W. Buckel, "Superconductivity in the Palladium-Hydrogen and the Palladium-Deuterium Systems," *Z. Phys.*, *257*, 1-8 (1972). (Equi Diagram; Experimental)

72Wis: M.L.H. Wise, J.P.G. Farr, I.R. Harris, and J.R. Hirst, "Transformations in Palladium-Hydrogen Alloys," *International Congress on Hydrogen in Metals*, Vol. I, Editions Science et Industrie, Paris, 72-75 (1972). (Equi Diagram; Experimental)

73Bur: R. Burch and N.B. Francis, "Pressure Against Composition Isotherms and Thermodynamic Data for the alpha-Phase of the Palladium/Hydrogen System," *J. Chem. Soc., Faraday Trans. I*, *69*, 1978-1982 (1973). (Equi Diagram, Thermo; Experimental)

73Cle: J.D. Clewley, T. Curran, T.B. Flanagan, and W.A. Oates, "Thermodynamic Properties of Hydrogen and Deuterium Dissolved in Palladium at Low Concentrations over a Wide Temperature Range," *J. Chem. Soc. Faraday Trans. I*, *69*, 449-458 (1973). (Equi Diagram, Thermo; Experimental)

73Fri: H. Frieske and E. Wicke, "Magnetic Susceptibility and Equilibrium Diagram of PdHn," *Ber. Bunsenges. Phys. Chem.*, *77*(1), 48-52 (1973). (Equi Diagram; Experimental; #)

73Hal: C.K. Hall and G. Stell, "Phase Transitions in Two Dimensional Lattice Gases of Hard-Core Molecules with Long-Range Attractions," *Phys. Rev. A*, *7*, 1679-1689 (1973). (Equi Diagram; Theory; #)

73Kha: A.G. Khachaturyan, "The Problem of Symmetry in Statistical Thermodynamics of Substitutional and Interstitial Ordered Solid Solutions," *Phys. Status Solidi (b), 60*, 9-37 (1973). (Crys Structure; Theory)

74Buc: R.V. Bucur and T.B. Flanagan, "The Effect of the Absorption of Hydrogen and Deuterium on the Frequency of a Quartz-Palladium Resonator," *Z. Phys. Chem., Neue Folge, 88*, 225-241 (1974). (Equi Diagram; Experimental)

74Eva: M.J.B.Evans, "Surface Area Effects on the Sorption of Hydrogen by Palladium," *Can. J. Chem., 52*, 1200-1205 (1973). (Equi Diagram; Experimental)

74Har: J.M.E. Harper, "The Effect of Hydrogen Concentration on Superconductivity and Clustering in Palladium Hydride," *Phys. Lett. A, 47*, 69-70 (1974). (Equi Diagram; Experimental)

74Hor: H. Horner and H. Wagner, "A Model Calculation for the alpha-alpha Phase Transition in Metal Hydrogen Systems," *J. Phys. C, Solid State Phys., 7*, 3305-3325 (1974). (Equi Diagram, Thermo; Theory)

74Lyn: J.F. Lynch and T.B. Flanagan, "Calorimetric Determination of Differential Heats of Absorption of Hydrogen by Palladium," *J. Chem. Soc. Faraday Trans. I, 70*, 814-821 (1974). (Thermo; Experimental)

74Mac: C.A. Mackliet, D.J. Gillespie, and A.I. Schindler, "Specific Heat of Superconducting Pd-H Alloys," *Solid State Commun., 15*, 207-210 (1974). (Thermo; Experimental)

74Rib1: Y. de Ribaupierre and F.D. Manchester, "Experimental Study of the Critical-Point Behaviour of the Hydrogen in Palladium System: I. Lattice Gas Aspects," *J. Phys. C, Solid State Phys., 7*, 2126-2139 (1974). (Equi Diagram, Crys Structure, Thermo; Experimental)

74Rib2: Y. de Ribaupierre and F.D. Manchester, "Experimental Study of the Critical-Point Behaviour of the Hydrogen in Palladium System: II. Specific Heat," *J. Phys. C, Solid State Phys., 7*, 2140-2146 (1974). (Equi Diagram, Thermo; Experimental)

74Sta: S.W. Stafford and R. McLellan, "Specific Heat Anomalies in Metal Hydrides," *Acta Metall., 22*, 1391-1395 (1974). (Thermo; Theory)

74Wag: H. Wagner and H. Horner, "Elastic Interaction and the Phase Transition in Coherent Metal-Hydrogen Systems," *Adv. Phys., 33*, 587-637 (1974). (Equi Diagram, Thermo; Theory)

75Fla1: T.B. Flanagan, J.F. Lynch, and J.D. Clewley, "Hydrogen Solubility as a Probe for Monitoring Recovery in Palladium," *Scr. Metall., 9*, 1063-1068 (1975). (Equi Diagram; Experimental)

75Fla2: T.B. Flanagan and J.F. Lynch, "Thermodynamics of a Gas in Equilibrium with Two Nonstoichiometric Condensed Phases. Application to Metal/Hydrogen Systems," *J. Phys. Chem., 79*(5), 444-448 (1975). (Thermo; Theory)

75Fla3: T.B. Flanagan, J.D. Clewley, and J.F. Lynch, "The Effect of Dislocations on the Hydride Phase Transition in the Palladium/Hydrogen System," *J. Less-Common Met., 41*, 343-346 (1975). (Equi Diagram; Experimental)

75Fon: D. de Fontaine, "k-Space Symmetry Rules for Order-Disorder Reactions," *Acta Metall., 23*, 553-571 (1975). (Crys Structure; Theory)

75Mue: M. Mueller, J. Faber, H.E. Flotow, and D.G. Westlake, "Studies on Nonstoichiometric PdHX," *Bull. Am. Phys. Soc., 20*, 421 (1975). (Crys Structure; Experimental)

75Oat: W.A. Oates and T.B. Flanagan, "The Reaction of Hydrogen Atoms with Palladium and its Alloys," *Can. J. Chem., 53*, 694-701 (1975). (Equi Diagram; Experimental)

75Rib: Y. de Ribaupierre and F.D. Manchester, "Experimental Study of the Critical-Point Behaviour of the Hydrogen in Palladium System: III. Spinodal Curves and Isotherm Relations," *J. Phys. C, Solid State Phys., 8*, 1339-1348 (1975). (Equi Diagram; Experimental; #)

75Sch: J.E. Schirber and B. Morosin, "Lattice Constant of beta-PdH_x and beta-PdD_x with X near 1.0," *Phys. Rev. B, 12*, 117-118 (1975). (Equi Diagram, Crys Structure; Experimental)

76Bir: H.K. Birnbaum, M.L. Grossbeck, and M. Amano, "Hydride Precipitation in Nb and Some Properties of NbH," *J. Less-Common Met., 49*, 357-370 (1976). (Equi Diagram; Experimental)

76Bou1: G. Boureau, O.J. Kleppa, and P. Dantzer, "High-Temperature Thermodynamics of Palladium-Hydrogen. I. Dilute Solutions H2 and D2 in Pd at 555 K," *J. Chem. Phys., 64*(12), 5247-5254 (1976). (Equi Diagram, Thermo; Experimental)

76Bou2: G. Boureau and O.J. Kleppa, "High-Temperature Thermodynamics of Palladium-Hydrogen. II. Temperature Dependence of Partial Molar Properties of Dilute Solutions of Hydrogen in the Range 500-700 K," *J. Chem. Phys., 65*, 3915-3920 (1976). (Equi Diagram, Thermo; Experimental)

76Eva: M.J.B. Evans and D.H. Everett, "Thermodynamics of the Solution of Hydrogen and Deuterium in Palladium," *J. Less-Common Met., 49*, 123-145 (1976). (Thermo; Experimental)

76Fla1: T.B. Flanagan, J.F. Lynch, J.D. Clewley, and B. von Turkovich, "The Effect of Lattice Defects on Hydrogen Solubility in Palladium. I. Experimentally Observed Solubility Enhancements and Thermodynamics of Absorption," *J. Less-Common Met., 49*, 13-24 (1976). (Equi Diagram; Experimental)

76Fla2: T.B. Flanagan and J.F. Lynch, "The Effect of Lattice Defects on Hydrogen Solubility in Palladium. II. Interpretation of Solubility Enhancements," *J. Less-Common Met., 49*, 25-35 (1976). (Equi Diagram; Experimental)

76Fro: "Gases and Carbon in Metals," E. Fromm and E. Gebhardt, Ed., Springer-Verlag, New York (1976). (Compilation)

76Hun: D.G. Hunt and D.K. Ross, "Optical Vibrations of Hydrogen in Metals," *J. Less-Common Met., 49*, 169-171 (1976). (Crys Structure, Thermo; Experimental)

76Jac1: J.K. Jacobs, C.R. Brown, V.S. Pavlov, and F.D. Manchester, "The '50 K' Transition in Palladium-Hydrogen Alloys: I. Internal Friction," *J. Phys. F, Met. Phys., 6*, 2219-2232 (1976). (Equi Diagram, Thermo; Experimental)

76Jac2: J.K. Jacobs and F.D. Manchester, "Thermal and Motional Aspects of the 50 K Transition in PdH and PdD," *J. Less-Common Met., 49*, 67-73 (1976). (Equi Diagram; Experimental)

76Jac3: N. Jacobi and R.W. Vaughan, "The 55 K Specific Heat Anomaly in Palladium Hydride," *Scr. Metall., 10*, 437-439 (1976). (Thermo; Theory)

76Jam: H.C. Jamieson, G.C. Weatherly, and F.D. Manchester, "The beta → alpha Phase Transformation in Palladium-Hydrogen Alloys," *J. Less-Common Met., 50*, 85-102 (1976). (Equi Diagram, Crys Structure; Experimental)

76Mac: C.A. Mackliet, D.J. Gillespie, and A.I. Schindler, "Specific Heat, Electrical Resistance, and Other Properties of Superconducting Pd-H Alloys," *J. Phys. Chem. Solids, 37*, 379-388 (1976). (Thermo; Experimental)

76Man: F.D. Manchester, "Lattice Gas Aspects of Metal-Hydrogen Systems," *J. Less-Common Met., 49*, 1-12 (1976). (Equi Diagram; Review)

76Miz: U. Mizutani, T.B. Massalski, and J. Bevk, "Low Temperature Specific Heats in Dilute Pd-H Alloys," *J. Phys. F, Met. Phys., 6*, 1-9 (1976). (Thermo; Experimental)

76Zim: G.J. Zimmermann, "Internal Friction and Modulus Behaviour of PdHn with H-Contents up to n = 0.9," *J. Less-Common Met., 49*, 49-66 (1976). (Equi Diagram; Experimental)

77Als: J. Als-Nielsen and R.J. Birgeneau, "Mean Field Theory, the Ginzburg Criterion, and Marginal Dimensionality of Phase Transitions," *Am. J. Phys., 45*, 554-560 (1977). (Equi Diagram; Theory)

77Bou: G. Boureau and O.J. Kleppa, "A Conjecture On a Possible Relation Between the 55 K Heat Capacity Anomaly in Palladium Hydride and the Modification of the Vibrational Spectrum of Palladium," *Scr. Metall., 11*, 327-329 (1977). (Thermo; Theory)

77Dek: I.Ya. Dekhtyar, M.M. Nishchenko, V.M. Pan, A.D. Shevchenko, and V.I. Schevchenko, "Magnetic Susceptibility of the Pd-H System

in the 4.2-300 K Range," *Fiz. Tverd. Tela, 19*, 881-882 (1977) in Russian; TR: *Sov. Phys. Solid State, 19*, 511-512 (1977). (Equi Diagram, Thermo; Experimental)

77Ho: E.T.C. Ho, H.A. Goldberg, G.C. Weatherly, and F.D. Manchester, "The beta → alpha Transformation in Palladium-Hydrogen Alloys," *Second Int'l Congress on Hydrogen in Metals*, 2B3, June 6-11, Paris, France 1-8, Pergamon, Oxford (1977). (Equi Diagram, Crys Structure; Theory)

77Jac: J.K. Jacobs and F.D. Manchester, "The 50 K Transition in Palladium-Hydrogen Alloys: II Specific Heat and Thermal Relaxation," *J. Phys. F, Met. Phys., 7*, 23-33 (1977). (Equi Diagram, Thermo; Experimental)

77Lyn: J.F. Lynch, J.D. Clewley, T. Curran, and T.B. Flanagan, "The Effect of the alpha-beta Phase Change on the alpha Phase Solubility of Hydrogen in Palladium," *J. Less-Common Met., 55*, 153-163 (1977). (Equi Diagram; Experimental)

77Mag: A. Magerl, N. Stump, H. Wipf, and G. Alefeld, "Interstitial Position of Hydrogen in Metals from Entropy of Solution," *J. Phys. Chem. Solids, 38*, 683-686 (1977). (Thermo; Experimental)

77Miz: U. Mizutani, T.B. Massalski, J. Bevk, and R.R. Vandervoort, "Influence of Deformation on the Low-Temperature Specific Heat of a Dilute alpha-Phase Pd-H Alloy," *J. Phys. F, Met. Phys., 7*, 3, L63-L68 (1977). (Thermo; Experimental)

78And1: I.S. Anderson, C.J. Carlile, and D.K. Ross, "The 50 K Transition in beta-Phase Palladium Deuteride Observed by Neutron Scattering," *J. Phys. C, Solid State Phys., 11*, L381-L384 (1978). (Equi Diagram, Crys Structure; Experimental)

78And2: I.S. Anderson, D.K. Ross, and C.J. Carlile, "The Structure of the gamma Phase of Palladium Deuteride," *Phys. Lett. A, 68*, 249-251 (1978). (Equi Diagram, Crys Structure; Experimental)

78Bar: B. Baranowski, "Metal-Hydrogen Systems at High Hydrogen Pressures," *Hydrogen in Metals II, Topics in Applied Phys.*, G. Alefeld and J. Volkl, Ed., Springer Verlag, Berlin, Vol. 29, 157-198 (1978). (Equi Diagram; Review)

78Bou2: G. Boureau and G.J. Kleppa, "Reply to Rush and Rowe's Comments," *J. Chem. Phys., 68*, 3955 (1978). (Thermo; Theory)

78Far: R.J. Farraro and R.B. McLellan, "Elastic Properties of Dilute Palladium-Hydrogen Solid Solutions," *J. Phys. Chem. Solids, , 39*, 781-785 (1978). (Thermo; Experimental)

78Gol1: H.A. Goldberg and F.D. Manchester, "Low Temperature Ordering in Pd-Hx (Dx) Alloys," *Phys. Lett. A, 68*, 360-362 (1978). (Crys Structure; Theory)

78Gol2: H.A. Goldberg, "Model Possibilities for the 50 K Transition in Pd-H_x," *Transition Metals, Conference Series 39*, Inter. Conf. on Transition Metals, Toronto, 15-19 Aug. 1977, The Institute of Physics, Bristol and London, 504-507 (1978). (Equi Diagram, Crys Structure; Theory)

78Hir: J.P. Hirth and B. Carnahan, "Hydrogen Adsorption at Dislocations and Cracks in Fe," *Acta Metall., 26*, 1795-1803 (1978). (Equi Diagram, Thermo; Theory)

78Kin: H.W. King and F.D. Manchester, "A Low Temperature X-Ray Diffraction Study of Pd and Some Pd-H Alloys," *J. Phys. F, Met. Phys., 8*, 15-25 (1978). (Equi Diagram, Crys Structure; Experimental)

78Lab: C. Labes and R.B. McLellan, "Thermodynamic Behaviour of Dilute Palladium-Hydrogen Solid Solutions," *Acta Metall., 26*, 893-899 (1978). (Thermo; Experimental)

78Mil: R.J. Miller, T.O. Brun, and C.B. Satterthwaite, "Magnetic Susceptibility of Pd-H and Pd-D at Temperatures Between 6 and 150 K," *Phys. Rev. B, 18*, 5054-5058 (1978). (Equi Diagram, Crys Structure; Experimental)

78Pic: C. Picard, O.J. Kleppa, and G. Boureau, "A Thermodynamic Study of the Palladium-Hydrogen System at 245-352 °C and at Pressures up to 34 atm.," *J. Chem. Phys., 69*, 5549-5556 (1978). (Equi Diagram, Thermo; Experimental)

78Rud: P.S. Rudman, "Thermodynamics of Pressure Plateaus in Metal-Hydrogen Systems," *Int. J. Hydrogen Energy, 3*, 431-447 (1978). (Equi Diagram, Thermo; Theory)

78Rus: J.J. Rush and J.M. Rowe, "Comment on 'High Temperature Thermodynamics of Palladium-Hydrogen. II. Temperature Dependence of Partial Molar Properties of Dilute Solutions of Hydrogen in the Range 500-700 K' *J. Chem. Phys., 65*, 3915 (1976)]" *J. Chem. Phys., 68*(8), 3954-3955 (1978). (Thermo; Experimental)

78Str: B. Stritzker and H. Wuhl, "Superconductivity in Metal-Hydrogen Systems", *Topics in Applied Physics*, Vol. 29, *Hydrogen in Metals II*, G. Alefeld and J. Volkl, Ed., Springer-Verlag, Berlin 243-272, (1978). (Equi Diagram, Crys Structure; Review)

78Swi: A.C. Switendick, "The Change in Electronic Properties on Hydrogen Alloying and Hydride Formation," *Hydrogen in Metals I*, G. Alefeld and J. Volkl, Ed., Springer-Verlag, New York, 101-130 (1978). (Crys Structure; Review)

78Web: R.A. Webb, J.B. Ketterson, W.P. Halperin, J.J. Vuillemin, and N.B. Sandesara, "Very Low Temperature Search for Superconductivity in Pd, Pt, and Rh," *J. Low Temp. Phys., 32*, 659-664 (1978). (Equi Diagram; Experimental)

78Wic: E. Wicke, H. Brodowsky, and H. Zuchner, "Hydrogen in Palladium and Palladium Alloys," *Hydrogen in Metals II*, G. Alefeld and J. Volkl, Ed., Springer-Verlag, New York, 73-156 (1978). (Thermo; Review; #)

79Die: S. Dietrich and H. Wagner, "Model Calculation for the Incoherent Phase-Transition in the Palladium-Hydrogen System," *Z. Phys. B, 36*, 121-126 (1979). (Equi Diagram; Theory; #)

79Ell: T.E. Ellis and C.B. Satterthwaite, "Evidence for H(D) Ordering in PdH_x (PdD_x)," *Phys. Rev. Lett., 42*, 7, 456-458 (1979). (Equi Diagram, Crys Structure; Experimental)

79Eve: D.H. Everett and P.A. Sermon, "Crystallite Size Effects in the Palladium/Hydrogen System: A Simultaneous Sorption and X-Ray Study," *Z. Phys. Chem. Neue Folge, 109*, 109-122 (1979). (Equi Diagram, Crys Structure; Experimental)

79Fra: G.A. Frazier and R.Glosser, "Phase Diagrams of Thin Films of the Palladium Hydrogen System Using a Quartz Crystal Thickness Monitor," *J. Phys. D, 12*, L113-115 (1979). (Equi Diagram; Experimental)

79Ho: E.C. Ho, H.A. Goldberg, G.C. Weatherly, and F.D. Manchester, "An In Situ Electron Microscope Study of Precipitation in Palladium-Hydrogen Alloys," *Acta Metall., 27*, 841-853 (1979). (Equi Diagram, Crys Structure, Thermo; Experimental)

79Hsu: D.K. Hsu and R.G. Leisure, "Elastic Constants of Palladium and beta-Palladium Hydride Between 4 and 300 K," *Phys. Rev. B, 20*, 1339-1344 (1979). (Equi Diagram; Experimental)

79Kep: J.B. Kepka and E.W. Czaputowicz, "Analysis of Some Results on Pd-H and Ni-H Systems Studied in High-Pressure-Hydrogen Condition," *Phys. Rev. B, 19*(4), 2414-2416 (1979). (Equi Diagram; Experimental)

79Lew: F.A. Lewis, W.D. McFall, and T.C. Witherspoon, "Hysteresis of Pressure-Composition and Electrical Resistance-Composition Relationships of Palladium Alloy/Hydrogen Systems," *Z. Phys. Chem., Neue Folge, 114*, 239-249 (1979). (Equi Diagram; Experimental)

79Sta: R.W. Standley, M. Steinback, and C.B. Satterthwaite, "Superconductivity in $PdH_x(D_x)$ from 0.2 to 4K," *Solid State Commun., 31*, 801-804 (1979). (Equi Diagram; Experimental)

79Swi: A.C. Switendick, "Band Structure Calculations for Metal-Hydrogen Systems," *Z. Phys. Chem., Neue Folge, 117*, 89-100 (1979). (Equi Diagram; Theory)

80Bla: O. Blaschko, R. Klemencic, and P. Weinzierl, "Structural Changes in PdD_x in the Temperature Region of the 50K Anomaly," *Acta Crystallogr. A, 36*, 605-609 (1980). (Crys Structure; Experimental)

80Fla: T.B. Flanagan, B.S. Bowerman, and G.E. Biehl, "Hysteresis in Metal/Hydrogen Systems," *Scr. Met., 14*, 443-447 (1980). (Equi Diagram, Thermo; Experimental)

80Fra: G.A. Frazier and R. Glosser, "Characterization of Thin Films of the Palladium-Hydrogen System," *J. Less-Common Met.*, *74*, 89-96 (1980). (Equi Diagram; Experimental)

80Kal: N.N. Kalinyuk, "Solubility of Hydrogen in Solid and in Liquid Palladium," *Zh. Fiz. Khim.*, *54*, 2815-2818 (1980) in Russian; TR: *Russ. J. Phys. Chem.*, *54*, 1611-1613 (1980). (Equi Diagram; Experimental)

80Lan: L.D. Landau and E.M. Lifshitz, *Statistical Physics*, Part I, Pergamon, Oxford, Ch. 1 (1980). (Thermo; Review)

80San: J.M. Sanchez and D. deFontaine, "Ordering in fcc Lattices with First- and Second Neighbor Interactions," *Phys. Rev. B*, *21*, 216-228 (1980). (Crys Structure; Theory; #)

80Sem: S.A. Semiletov, R.V. Baranova, Yu.P. Khodyrev, and R.M. Imamov, "Electron-Diffraction Investigation of Tetragonal $PdH_{1.33}$," *Kristallografiya*, *25*, 1162-1168 (1980) in Russian; TR: *Sov. Phys. Crystallogr.*, *25*, 665-669 (1980). (Equi Diagram, Crys Structure; Experimental)

80Tys: W.R. Tyson, "The Effect of Lattice Defects on Hydrogen Solubility," *J. Less-Common Met.*, *70*, 209-212 (1980). (Equi Diagram; Theory)

81Bar: R.I. Barabash and M.A. Krivoglaz, "Influence of Anisotropy on X-Ray Scattering by Highly Distorted Ageing Solid Solutions," *Phys. Met. Metallogr.*, *51*, 903-916 (1981). in Russian; TR: *Phys. Met. Metallogr.*, *51*, 1-12 (1981). (Crys Structure; Theory)

81Bla: O. Blaschko, P. Fratzl, and R. Klemencic, "Model for the Structure Changes Occurring at Low Temperatures in PdD_x," *Phys. Rev. B*, *24*, 277-282 (1981). (Equi Diagram, Crys Structure; Experimental)

81Bon: R.A. Bond, D.K. Ross, I.S. Anderson, and C.J. Carlile, "Neutron Diffraction Studies of the Time Dependence of the 50 K Transition in alpha' Pd/D," *Physics of Transition Metals*, Conference Series Number 55, Intern. Conf. on the Physics of Transition Metals, Leeds, England, 18-22 Aug. 1980, The Institute of Physics, Bristol and London, 379-382 (1981). (Crys Structure; Experimental)

81Her: C. Herrero and F.D. Manchester, "Location of the Low Temperature Resistivity Anomaly in Pd-D," *Phys. Lett. A*, *86*, 29-31 (1981). (Crys Structure; Experimental)

81Kir1: R. Kirchheim, "Interaction of Hydrogen with Dislocations in Palladium—I. Activity and Diffusivity and their Phenomenological Interpretation," *Acta Metall.*, *29*, 835-843 (1981). (Equi Diagram; Experimental)

81Kir2: R. Kirchheim, "Interaction of Hydrogen with Dislocations in Palladium—II. Interpretation of Activity Results by a Fermi-Dirac Distribution," *Acta Metall.*, *29*, 845-853 (1981). (Equi Diagram, Thermo; Experimental)

81Maz: F.M. Mazzolai, P.G. Bordoni, and F.A. Lewis, "Elastic Energy Dissipation Effects in alpha+beta and beta Phase Composition Ranges of the Palladium-Hydrogen System," *J. Phys. F, Met. Phys.*, *11*, 337-352 (1981). (Equi Diagram; Experimental)

81Sak: Y. Sakamoto and N. Tabaru, "Diffusivity and Solubility of Hydrogen in Annealed and Cold Rolled Specimens of Palladium," *J. Jpn. Inst. Met.*, *45*, 1048-1055 (1981) in Japanese. (Equi Diagram; Experimental)

81Wic: E. Wicke and J. Blaurock, "Equilibrium and Susceptibility Behaviour of the Pd/H_2 System in the Critical and Supercritical Region," *Ber. Bunsenges. Chem.*, *85*, 1091-1096 (1981). (Thermo; Experimental)

82Bon: R.A. Bond and D.K. Ross, "The Use of Monte Carlo Simulations in the Study of a Real Lattice Gas and its Application to the alpha' Pd-D System," *J. Phys. F, Met. Phys.*, *12*, 597-609 (1982). (Equi Diagram, Crys Structure; Theory; #)

82Fla: T.B. Flanagan and J.D. Clewley, "Hysteresis in Metal-Hydrides," *J. Less-Common Met.*, *83*, 127-141 (1982). (Thermo; Theory)

82Kir: R. Kirchheim, "Interaction of Hydrogen with Dislocations," *Proc. Adv. Tech. Charact. Hydrogen Met. Symposium*, N.F. Fiore and B.J. Berkowitz, Ed., Metallurgical Society AIME, Warrendale, PA, 77-86 (1982). (Equi Diagram, Thermo; Experimental)

82Kle: O.J. Kleppa and R.C. Phutela, "A Calorimetric-Equilibrium Study of Dilute Solutions of Hydrogen and Deuterium in Palladium at 555 to 909K," *J. Chem. Phys.*, *76*, 1106-1110 (1982). (Thermo; Experimental)

83Bak: H.L.M. Baker, G.J. de Bruin-Hordijk, R. Feenstra, R. Griessen, D.G. de Groot, and J. Rector, "Hydrogen Absorption and Critical Point Lowering in Thin PdH_x Films," *Electronic Structure and Properties of Hydrogen in Metals*, Nato Conference Series VI: Materials Science, Vol. 6, P. Jena and C.B. Satterthwaite, Ed., Plenum Press, New York, 659-664 (1983). (Equi Diagram; Experimental)

83Bal: I.S.L. Balbaa and F.D. Manchester, "Superconductivity of PdH_x in Relation to its Phase Diagram: Magnetic Measurements," *J. Phys. F, Met. Phys.*, *13*, 395-404 (1983). (Equi Diagram, Crys Structure; Experimental)

83Bon: R.A. Bond, I.S. Anderson, B.S. Bowerman, C.J. Carlile, D.J. Picton, D.K. Ross, D.G. Witchell, and J.K. Kjems, "Neutron Diffraction Studies of the Low Temperature Transition in alpha' PdD," *Electronic Structure and Properties of Hydrogen in Metals*, NATO Conference Series VI: Materials Science, Vol. 6, P. Jena and C. Satterthwaite, Ed., Plenum Press, New York, 189-195 (1983). (Equi Diagram, Crys Structure; Experimental)

83Fee: R. Feenstra, G.J. de Bruin-Hordijk, H.L.M. Bakker, R. Griessen, and D.G. de Groot, "Critical Point Lowering in Thin PdH_x Films," *J. Phys. F, Met. Phys.*, *13*, L13-L18 (1983). (Equi Diagram; Experimental; #)

83Fla: T.B. Flanagan and W.A. Oates, "The Effect of Hysteresis on the Phase Diagram of Pd-H," *J. Less-Common Met.*, *92*, 132-142 (1983). (Equi Diagram; Experimental)

83Kuj: T. Kuji, W.A. Oates, B.S. Bowerman, and T.B. Flanagan, "The Partial Excess Thermodynamic Properties of Hydrogen in Palladium", *J. Phys. F, Met. Phys*, *13*, 1785-1800 (1983). (Thermo; Experimental)

83Las: R. Lasser and K.-H. Klatt, "Solubility of Hydrogen Isotopes in Palladium," *Phys. Rev. B*, *28*, 748-758 (1983). (Equi Diagram, Thermo; Experimental)

83Sta: R.W. Standley and C.B. Satterthwaite, "Effect of Structural Phase Transitions on the Superconductivity of $PdH_x(D_x)$," *Electronic Structure and Properties of Hydrogen in Metals*, P. Jena and C.B. Satterthwaite, Ed., Plenum Press, New York, 335-340 (1983). (Crys Structure; Experimental)

84Bal: I.S. Balbaa, A.J. Pindor, and F.D. Manchester, "Superconductivity of PdH_x in Relation to its Phase Diagram. II. Specific Heat Measurements and the Form of the $T_c(X)$ Relation," *J. Phys. F, Met. Phys.*, *14*, 2637-2647 (1984). (Equi Diagram, Crys Structure; Experimental)

84Bla1: O. Blashko, "Structural Features Occurring in PdD_x Within the 50 K Anomaly Region," *J. Less-Common Met.*, *100*, 307-320 (1984). (Crys Structure; Experimental)

84Bla2: O. Blaschko, "Fermi Surface Imaging Effect in the D Short-Range Order of PdD_x," *Phys. Rev. B*, *29*, 5187-5189 (1984). (Equi Diagram; Theory; #)

84Gee: B.M. Geerken, H. Hemmes, and R. Griessen, "Influence of the 50K Phase Transition on the Thermal Expansion and Electrical Resistivity of the alpha' Pd-H_x," *J. Phys. F, Met. Phys.*, *14*, 813-822 (1984). (Equi Diagram; Experimental)

84Gri: R. Griessen and A. Driessen, "Heat of Formation and Band Structure of Binary and Ternary Metal Hydrides," *Phys. Rev. B*, *30*, 4372-4381 (1984). (Thermo; Theory)

84Hem: H. Hemmes, B.M. Geerken, and R. Griessen, "Contribution of Optical Phonons to the Thermal Expansion of alpha' PdH_x and alpha'-PdD_x," *J. Phys. F, Met. Phys.*, *14*, 2923-2933 (1984). (Equi Diagram, Thermo; Experimental)

84Las: R. Lasser, "Solubility of Protium, Deuterium, and Tritium in the alpha Phase of Palladium," *Phys. Rev. B*, *29*, 4765-4768 (1984). (Equi Diagram, Thermo; Experimental)

85Bla: J.G. Blaurock, "Thermodynamics and Phase Diagram of the Pd/D_2 System in Comparison to Pd/H_2 and (the) Magnetic Behaviour of These Systems," thesis, Wilhelms-University, Munster, F.R.G. (1985) in German. (Equi Diagram, Thermo; Experimental; #)

85Las: R. Lasser, "Isotope Dependence of Phase Boundaries in the PdH, PdD, and PdT Systems," *J. Phys. Chem. Solids*, *46*, 33-37 (1985). (Equi Diagram; Experimental)

85Lee: Ming-Way Lee and R. Glosser, "Pressure Concentration Isotherms of Thin Films of the Palladium-Hydrogen System as Modified by Film Thickness, Hydrogen Cycling, and Stress," *J. Appl. Phys.*, *57*, 5236-5239 (1985). (Equi Diagram; Experimental)

85Wic: E. Wicke, "Some Present and Future Aspects of Metal-Hydrogen Systems," *Z. Phys. Chem., Neue Folge*, *44*, 1-21 (1985). (Equi Diagram, Thermo; Experimental)

86Fee1: R. Feenstra, R. Griessen, and D.G. de Groot, "Hydrogen Induced Lattice Expansion and Effective H-H Interaction in Single Phase PdH_c," *J. Phys. F, Met. Phys.*, *16*, 1933-1952 (1986). (Equi Diagram, Crys Structure, Thermo; Experimental)

86Fee2: R. Feenstra, D.G. de Groot, J.H. Rector, E. Salomons, and R. Griessen, "Gravimetrical Determinations of Pressure-Composition Isotherms of Thin PdHc Films," *J. Phys. F, Met. Phys.*, *16*, 1953-1963 (1986). (Equi Diagram, Experimental; #)

86Jon: S.E. Jones, "Muon-Catalysed Fusion Revisited," *Nature*, *321*, 127-133 (1986). (Equi Diagram; Review)

86Las: R. Lasser and G.L. Powell, "Solubility of H, D, and T in Pd at Low Concentration," *Phys. Rev. B*, *3*(2), 578-586 (1986). (Equi Diagram, Thermo; Experimental)

87Avr: H.E. Avram and R.L. Armstrong, "Low-Temperature Evolution of the Proton Magnetic Resonance Line Shape in beta-Phase Palladium Hydride," *J. Low Temp. Phys.*, *69*, 391-400 1987). (Equi Diagram; Experimental)

87Bal: I.S. Balbaa, P.A. Hardy, A. San-Martin, P.G. Coulter, and F.D. Manchester, "The Effect of Lattice Distortion on the X-Ray Measurements of Lattice Parameters for PdH_x: I. Empirical Relationships," *J. Phys. F, Met. Phys.*, *17*, 2041-2048 (1987). (Crys Structure; Experimental)

87Sal: E.M. Salomons, R. Feenstra, D.G. de Groot, J.H. Rector, and R. Griessen, "Pressure-Composition Isotherms of Thin PdH_c Films," *J. Less-Common Met.*, *130*, 415-420 (1987). (Equi Diagram; Experimental)

87Wic: E. Wicke and J. Blaurock, "New Experiments On and Interpretation of Hysteresis Effects of Pd-D_2 and Pd-H_2," *J. Less-Common Met.*, *130*, 351-363 (1987). (Equi Diagram; Experimental; #)

88Fla: T.B. Flanagan and C.-N. Park, "Hysteresis in Metal Hydrides," *Hydrogen Storage Materials*, R.G. Barnes, Ed., *Materials Science Forum*, *31*, 297-324 (1988). (Thermo; Review)

88Nyg: L.A. Nygren, C. Youngsin, D.K Hsu, and R.G. Leisure, "Density of Single-Crystal PdHx and PdDx in the alpha' Phase," *J. Phys. F, Met. Phys.*, *18*, 1127-1132 (1988). (Crys Structure; Experimental)

89Ben: M.J. Benham and D.K. Ross, "Experimental Determination of Absorption-Desorption Isotherms by Computer-Controlled Gravimetric Analysis," *Z. Phys. Chem., Neue Folge*, *163*, S25-32 (1989). (Equi Diagram; Experimental)

89Fla: T.B. Flanagan and T. Kuji, "Hysteresis in Metal Hydrides Evaluated From Data at Constant Hydrogen Content: Application to Palladium-Hydrogen," *J. Less-Common Met.*, *152*, 213-226 (1989). (Equi Diagram, Thermo; Experimental)

89Fle: M. Fleischmann and S. Pons, "Electrochemically Induced Nuclear Fusion of Deuterium," *J. Electroanal. Chem.*, *261*, 301-308 (1989). (Equi Diagram, Thermo; Experimental)

89Hem: H. Hemmes, A. Driessen, J. Kos, F.A. Mol, R. Griessen, J. Caro, and S. Radelaar, "Synthesis of Metal Hydrides and *in situ* Resistance Measurements in a High-Pressure Diamond Anvil Cell," *Rev. Sci. Inst.*, *60*, 474-480 (1989). (Equi Diagram; Experimental)

89Jon: S.E. Jones, E.P. Palmer, J.B. Czirr, D.L. Decker, G.L. Jensen, J.M. Thorne, S.F. Taylor, and J. Rafelski, "Observation of Cold Nuclear Fusion in Condensed Matter," *Nature*, *338*, 737-740 (1989). (Equi Diagram, Crys Structure, Thermo; Experimental)

89Ric: P.M. Richards, "Molecular Dynamics Investigation of Deuterium Separation in $PdD_{1.1}$," *Phys. Rev. B*, *40*, 7966-7968 (1989). (Equi Diagram, Crys Structure; Theory)

89Sun: Z. Sun and D. Tomanek, "Cold Fusion: How Close can Deuterium Atoms Come Inside Palladium?" *Phys. Rev. Lett.*, *63*, 59-61 (1989). (Equi Diagram, Crys Structure; Theory)

90Sil: I.F. Silvera and F. Moshary, "Deuterated Palladium at Temperatures from 4.3 to 400 K and Pressures to 105 kbar: Search for Cold Fusion," *Phys. Rev. B*, *42*, 9143-9146 (1990). (Equi Diagram; Experimental)

90Wei: S.-H. Wei and A. Zunger, "Stability of Atomic and Diatomic Hydrogen in fcc Palladium," *Solid State Commun.*, *73*, 327-330 (1990). (Equi Diagram, Crys Structure; Theory)

91Fla: T.B. Flanagan, W. Luo, and J.D. Clewley, "Calorimetric Enthalpies of Absorption and Desorption of Protium and Deuterium by Palladium," *J. Less-Common Met.*, *172-174*, 42-55 (1991). (Equi Diagram, Thermo; Experimental)

91Fuk: Y. Fukai, "From Metal Hydrides to the Metal-Hydrogen System," *J. Less-Common Met.*, *172-174*, 8-19 (1991). (Equi Diagram; Experimental)

91Hem: R. Hempelman, D. Richter, J.J. Rush, and J.M. Rowe, "Hydrogen Site Distribution in the Alloy System $Nb_{100-x}V_xH_y$ Studied by Neutron Vibrational Spectroscopy," *J. Less-Common Met.*, *172-174*, 281-292 (1991). (Thermo; Experimental)

91Pap: D.A. Papaconstantopoulos, J.P. Skroch, and G.D. Drew, "Calculations of the Total Energy, Electron-Phonon Interaction and Stoner Parameter in the 5d Transition Metal Hydrides," *J. Less-Common Met.*, *172-174*, 401-410 (1991). (Crys Structure; Theory)

91Ros: D.K. Ross, M.W. McKergow, D.G. Witchell, and J.K. Kjems, "Neutron Diffraction Studies of Domain Growth Associated with the 50K Anomaly in Pd-D," *J. Less-Common Met.*, *172-174*, 169-182 (1991). (Crys Structure; Experimental)

91Swi: A.C. Switendick, "Electronic Structure and Stability of Palladium Hydrogen (Deuterium) Systems, $PdH(D)_n$, $1 < n < 3$," *J. Less-Common Met.*, *172-174*, 1363-1370 (1991). (Equi Diagram, Crys Structure; Theory)

92San: M. Sandys-Wunsch and F.D. Manchester, "Spinodal Temperatures for Macroscopic Density Fluctuations in Pd-H: I & II," *J. Phys., Condens. Matter*, *4*, 2139-2154 (1992). (Equi Diagram; I: Theoretical, II: Experimental)

#Indicates presence of a phase diagram.

H-Pd evaluation contributed by **F.D. Manchester**, **A. San-Martin**, and **J.M. Pitre**, Centre for Metal Hydride Studies, McLennan Physical Laboratories, University of Toronto, Toronto, Ontario M5S 1A7, Canada. This work was supported by a grant from ASM International. Literature searched through 1991. Prof. Manchester is the Alloy Phase Diagram Program Co-Category Editor for binary hydrogen-metal alloys.